

### 3. PALEOGENE RADIOLARIANS FROM SITES 998, 999, AND 1001 IN THE CARIBBEAN<sup>1</sup>

Catherine Nigrini<sup>2</sup> and Annika Sanfilippo<sup>3</sup>

#### ABSTRACT

The Paleogene sequences from three sites in the Caribbean were examined for radiolarians. In general, samples are highly lithified, requiring lengthy and repetitive cleaning procedures, and the assemblages are usually fragmented and/or partially dissolved. Both abundances and preservation of the assemblages vary considerably from site to site and within a single site; even within a single sample more than one degree of preservation was observed. It was possible, however, to construct at least partial stratigraphies for each of the three sites. Because the abundance of radiolarians is high even in extremely poorly preserved assemblages, we conclude that the differences in biogenic silica preservation are the result of postdepositional processes and not productivity.

In both Sites 999 and 1001, near the Paleocene/Eocene boundary (*Bekoma bidartensis* Zone [RP7]), there is a short interval in which the abundance and preservation state of the radiolarians improves relative to overlying and underlying assemblages. In each case the intervals corresponds to the level, identified by calcareous microfossils, as representing changes in paleoceanographic conditions associated with the late Paleocene thermal maximum.

#### INTRODUCTION

Five sites were drilled in the Caribbean region during Ocean Drilling Program (ODP) Leg 165, but only three (Fig. 1) were examined for radiolarians. The main objectives of the leg were to examine the nature of the Cretaceous/Tertiary (K/T) boundary and to study the influence of tropical seas on global climate and ocean history. The initial Deep Sea Drilling Project (DSDP) policy of discontinuous coring yielded good, but intermittent, sequences from the Caribbean (Legs 4, 10, and 15). Given the superior drilling and continuous recovery now possible, it was thought that a reasonably good Paleogene radiolarian-bearing sequence might be obtained in this region. Hence, radiolarian samples were taken from Holes 998A, 998B, 999B, 1001A, and 1001B with the expectation that they would provide a continuous record of radiolarian deposition in the region. It was hoped that we could examine the paleoenvironmental signals provided by radiolarians during the interval surrounding the late Paleocene thermal maximum (LPTM) and that we could construct an integrated chronostratigraphy, using datum levels from radiolarians, calcareous microfossils, paleomagnetism, and isotopes, in and around critical, datable ash layers.

Unfortunately, the results have been disappointing in that radiolarian preservation is uneven and not as good as that found in earlier legs. Sample preparation proved to be both extremely difficult and time consuming, and the resulting assemblages are so poor that we were unable to make detailed biostratigraphic and taxonomic determinations. However, some partial stratigraphies could be constructed, and we have found a recognizable change in radiolarian abundance and preservation associated with the LPTM interval.

#### SAMPLE PREPARATION

To obtain clean radiolarian residues for microscopic examination, sediments must be disaggregated, sieved to remove the clay-size fraction, and acidified to eliminate the calcareous component (San-

filippo et al., 1985). Soft sediments are commonly disaggregated after being boiled in a solution of hydrogen peroxide and sodium pyrophosphate for a few minutes, but if lumps remain after sieving through a 63-µm (or 44 µm) mesh sieve, the coarse fraction is returned to the beaker, dried, and boiled again. Successive dryings and retreatments are sufficient to clean most radiolarian samples. The cleaned residue is sieved at 150, 63, and 44 µm and pipetted evenly onto labeled glass slides. When completely dry, air is expelled from the skeletons by the addition of a few drops of xylene, Canada balsam is dropped onto them, and a 22 mm × 44 mm coverslip completes the preparation.

Normally, lithologic smear slides of sediment samples will tell the observer whether or not radiolarians are present in the sample. Identification of radiolarians in the smear slides from this leg, especially from Hole 999B, is difficult because of the great degree of lithification and the overall scarcity of siliceous microfossils. In addition, most of the samples we obtained from Leg 165 were so highly lithified that disaggregation was difficult if not impossible. The standard method of radiolarian preparation for deep-sea sediments as described above was used, but most samples required repeated treatments (five to six times) with hydrogen peroxide and sodium pyrophosphate, sometimes over a period of days. We found it necessary to make many slides (up to 10 or more) from a single sample to find a sufficient number of well-preserved forms to make a stratigraphic determination. Many of our samples were barren of radiolarians. Frequently, volcanic glass shards and their alteration products, such as smectite, remain in the siliceous residues as minor constituents along with feldspar, opaque minerals, and traces of pyrite (P. Worstell, pers. comm., 1998).

#### RADIOLARIAN PRESERVATION

The Leg 165 assemblages show very poor preservation, and hence low diversity in the sediments, relative to previously reported assemblages of equivalent age from DSDP Legs 4 and 15 from the Caribbean and DSDP Leg 10 from the Gulf of Mexico. DSDP Leg 4 collected useful Caribbean middle Eocene sequences with radiolarians at Site 29 (Riedel and Sanfilippo, 1970) and Leg 15 provided Caribbean equivalents of the sediment sequences in the Gulf of Mexico (Riedel and Sanfilippo, 1973) which permitted correlation with calcareous microfossils. Leg 10 sampled a similar sequence (Foreman, 1973; Sanfilippo and Riedel, 1973) in the Gulf of Mexico. All of

<sup>1</sup>Leckie, R.M., Sigurdsson, H., Acton, G.D., and Draper, G. (Eds.), 2000. *Proc ODP, Sci. Results*, 165: College Station, TX (Ocean Drilling Program).

<sup>2</sup>161 Morris, Canmore, AB T1W 2W7, Canada. nigrini@idt.net

<sup>3</sup>Scripps Institution of Oceanography, University of California, San Diego, La Jolla, CA 92093-0220, U.S.A.

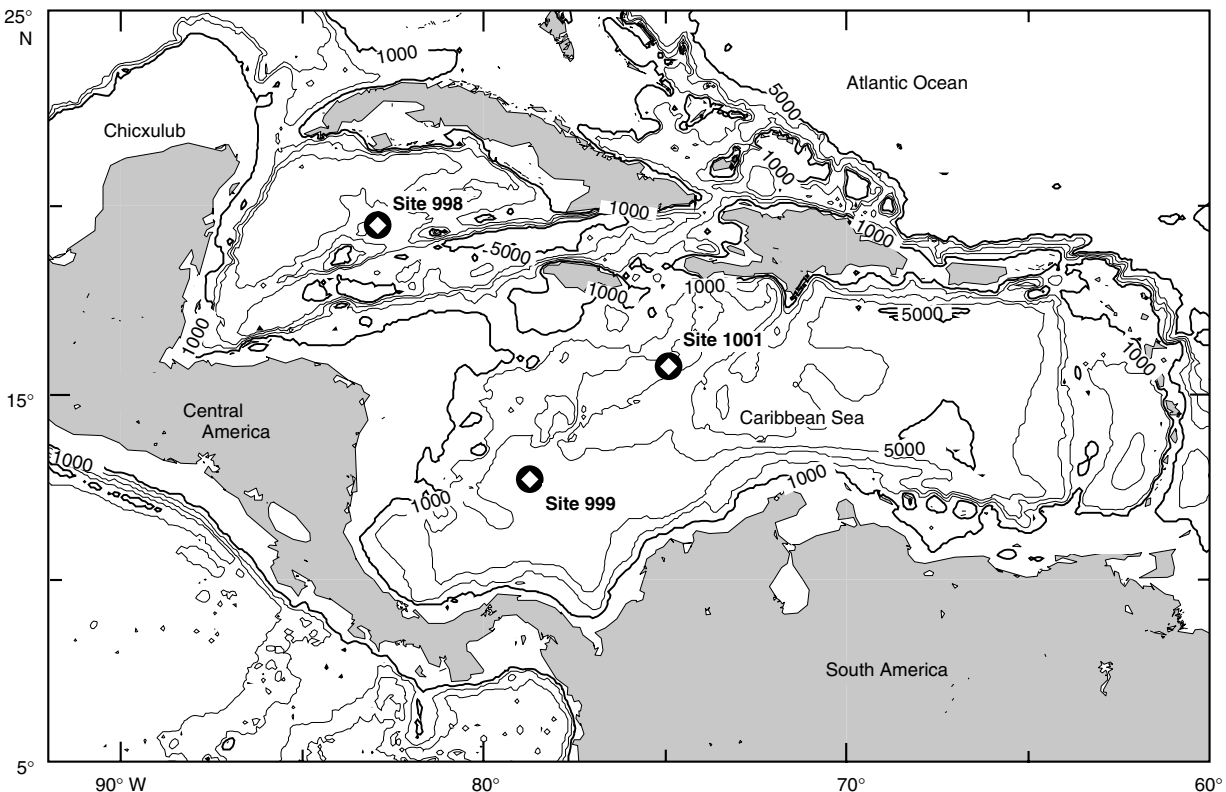


Figure 1. Location of Leg 165 sites examined for Paleogene radiolarians. Contours are in meters below sea level.

these legs lacked continuous coring from duplicate sites. Subsequent DSDP/ODP Legs (76–78, 96, 100–102, and 110) in the Caribbean region recovered only younger than middle Eocene radiolarian-bearing sediments. Although more numerous Paleocene and lower Eocene samples have been obtained from different parts of the world ocean, the recovery is still intermittent and radiolarian preservation commonly not adequate for detailed biostratigraphic work (Sanfilippo and Nigrini, 1998b). Other studies from this region have reported both very poor (Sanfilippo and Hull, in press) and relatively good (Florez Abin, 1983) preservation in Cuban land-based sections. Good preservation of Eocene material from Barbados was reported by Saunders et al. (1985), but preservation in other sections from Barbados (Sanfilippo, unpubl. data) is inconsistent and generally deteriorates with age.

Sporadically occurring well-preserved radiolarians in the Leg 165 sites (e.g., 165-999B-28R-1, 0–2 cm) represent assemblages characteristic of open-ocean conditions, but with notably less diversity. However, the following genera, which are of particular stratigraphic importance in low latitudes, are notably sparse or absent from the three sites investigated herein: *Podocyrtis*, *Thrysocyrtis*, and *Theotocyste*.

Not only do we see anomalous occurrences of well-preserved and poorly preserved assemblages within the region, we have also noted that, within a given site, and even with a given sample, the state of preservation is variable (Pl. 2, figs. 14–17; Pl. 3, figs. 11–13). For example, in Hole 999B the upper Eocene and Oligocene assemblages are composed of common, very poorly preserved radiolarians together with time-equivalent very rare but well-preserved forms, whereas the middle Eocene assemblage is characterized by abundant, very poorly preserved radiolarians that show evidence of strong dissolution. The upper Paleocene and lower Eocene assemblages are mostly barren of radiolarians except for sporadic occurrences of abundant, very poorly preserved forms. This observation suggests

that the absence of siliceous microfossils in sediments from this region is a result of dissolution within the sediment rather than the absence of specimens in the surface water.

The majority of our samples contain dissolved (Pl. 1, figs. 3, 9) and/or infilled radiolarian fragments or molds (Pl. 1, fig. 4). Frequently, diagnostic morphological features are missing (Pl. 1, figs. 5–7, 11), making identifications uncertain or impossible. In many of the nassellarians, dissolution is concentrated in the collar region (Pl. 2, fig. 11), which often results in the loss of the cephalis (Pl. 1, fig. 12). Even when specimens are sufficiently complete for identification, terminal segments, ornamentation, and spines are commonly missing or poorly preserved (Pl. 3). Fortunately, some forms have such a characteristic outline that they can be identified despite advanced dissolution or partial fragmentation (Pl. 1, figs. 8, 16; Pl. 2, figs. 3, 10). We have also observed that the refractive index of the silica in a few samples is lower (Pl. 1, fig. 10) than normal for Paleocene assemblages.

## RADIOLARIAN ZONATION

The code numbers for the Paleogene radiolarian zonation used herein are those introduced by Sanfilippo and Nigrini (1998a). In that paper we standardized and formally defined 39 radiolarian zones for the tropical Pacific, Indian, and Atlantic Oceans: RP1–RP22 for the Paleogene and RN1–RN17 for the Neogene. Mean numerical ages for zonal boundaries were culled from previous literature and converted to the geomagnetic polarity time scale of Cande and Kent (1995). A chart showing the correlation between the Paleogene zonal schemes for foraminifers, calcareous nannofossils, radiolarians, and the geomagnetic polarity time scale is shown in Figure 2. Below is a list of the zonal code numbers used herein, listed from youngest to oldest, which are equivalent to the previously published named zones.

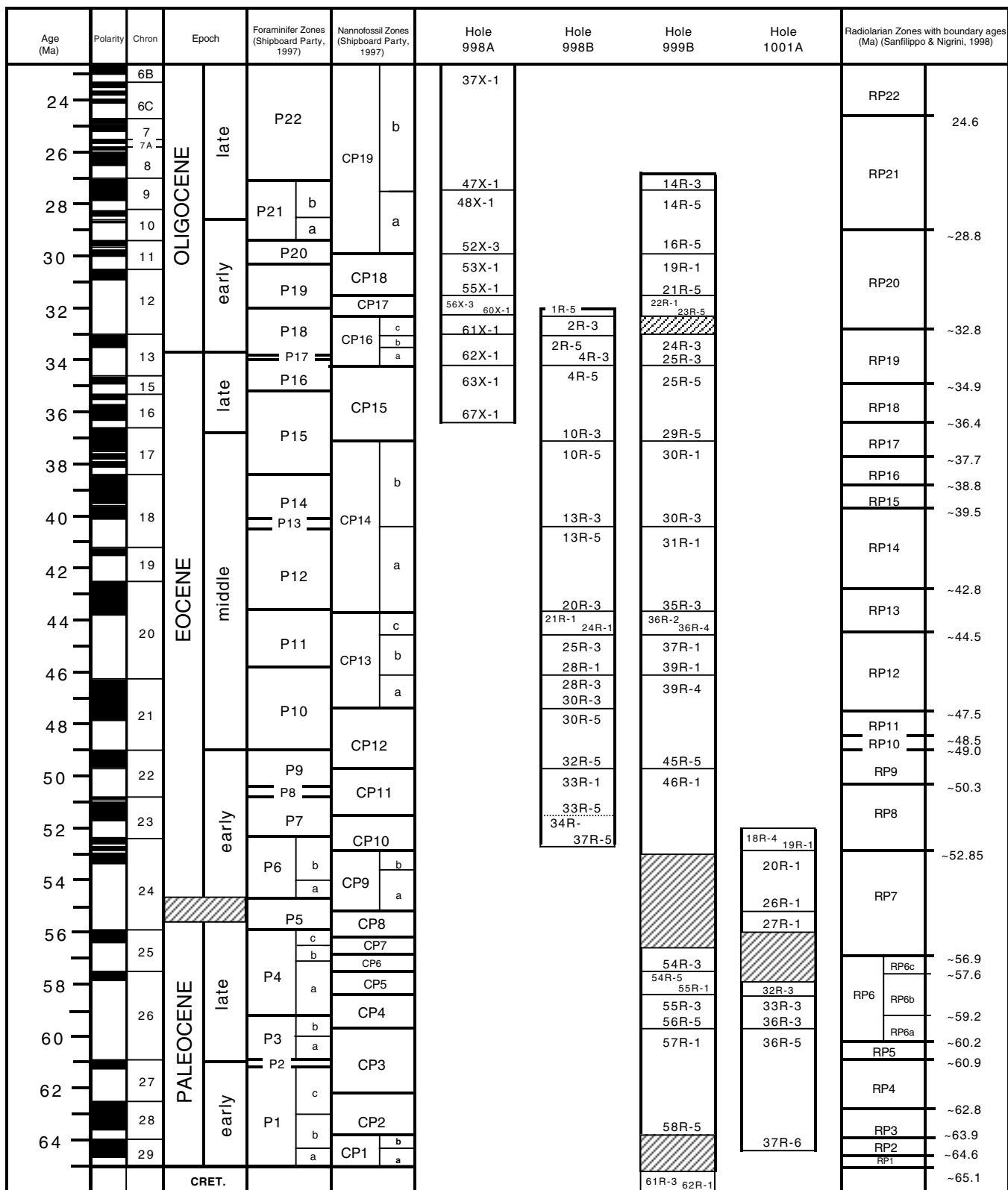


Figure 2. Correlation chart of Paleogene zonal schemes for foraminifers, calcareous nannofossils, radiolarians, and the geomagnetic polarity time scale of Cande and Kent (1995). Key to radiolarian zonal code numbers can be found in the text. Holes examined herein are correlated against nannofossil zones. Core and section numbers indicate level at which nannofossil boundaries occur. Hatching indicates uncertainty in placement of zonal boundary.

RP22	<i>Lychnocanoma elongata</i> Zone
RP21	<i>Dorcadospyris ateuchus</i> Zone
RP20	<i>Theocyrtis tuberosa</i> Zone
RP19	<i>Cryptocarpium ornatum</i> Zone
RP18	<i>Calocyclas bandycia</i> Zone
RP17	<i>Cryptocarpium azyx</i> Zone
RP16	<i>Podocyrtis (Lampterium) goetheana</i> Zone
RP15	<i>Podocyrtis (Lampterium) chalara</i> Zone
RP14	<i>Podocyrtis (Lampterium) mitra</i> Zone
RP13	<i>Podocyrtis (Podocyrtogetes) ampla</i> Zone
RP12	<i>Thyrsocyrtis (Pentalacorys) triacantha</i> Zone
RP11	<i>Dictyoprora mongolfieri</i> Zone
RP10	<i>Theocotyle cryptocephala</i> Zone
RP9	<i>Phormocyrtis striata striata</i> Zone
RP8	<i>Buryella clinata</i> Zone
RP7	<i>Bekoma bidartensis</i> Zone
RP6	<i>Bekoma campechensis</i> Zone
RP6c	<i>Stylotrochus nitidus–Pterocodon (?) poculum</i> Subzone
RP6b	<i>Orbula discipulus</i> Subzone
RP6a	<i>Peritiviator (?) dumitricai</i> Subzone
RP5	<i>Buryella tetradica</i> Zone
RP4	<i>Buryella foremanae</i> Zone
RP3	<i>Stichomitra granulata</i> Zone
RP2	<i>Amphisphaera kina</i> Zone
RP1	<i>Amphisphaera aotea</i> Zone

## SITE DESCRIPTIONS

### Site 998

#### Hole 998A

Hole 998A ( $19^{\circ}29.377'N$ ,  $82^{\circ}56.166'W$ ) was drilled on the Cayman Rise in 3179.9 m of water. Our samples (Table 1) were taken from between Samples 165-998A-36X-1, 36–38 cm (330.16 mbsf), and 67X-1, 4–6 cm (628.04 mbsf), which, according to nannofossil data, extends from the latest Oligocene (CN1a) to the late Eocene (CP15). All of our samples were highly calcareous and, except for the single sample (165-998A-36X-1, 36–38 cm) in nannofossil zonal equivalent CN1a and radiolarian zonal equivalent RP22, are either barren of radiolarians, or, at best, contain a few specimens of altered or broken forms. Despite the poor preservation, we were able to determine that Samples 165-998A-37X-1, 33–35 cm, to 45X-1, 89–91 cm, lie within radiolarian zonal equivalent RP21, Sample 165-998A-58X-3, 34–35 cm, lies within RP20 and Samples 165-998A-65X-1, 57–59 cm, and 67X-1, 4–6 cm, lie within RP18. These zonal assignments are in good agreement with those based on calcareous nannofossils.

#### Hole 998B

Hole 998B is a downward continuation of Hole 998A. Our samples (Table 2) were taken from between Samples 165-998B-1R-1, 38–40 cm (558.68 mbsf) and 37R-5, 35–37 cm (901.45 mbsf), which, according to nannofossil data, extends from the early Oligocene (CP17) to the early Eocene (CP10). Abundance is generally low in the lower Oligocene through the middle part of the middle Eocene, and it is mostly barren from below Sample 165-998B-26R-1, 34–36 cm (789.74 mbsf), where a substantial increase in dolomite content is noted. Sample 165-998B-34R-1, 35–37 cm, is tentatively assigned to radiolarian zonal equivalent RP8. Assignment of zonal equivalents to the remaining samples was sporadic and frequently tentative (see Table 2), but does, in general, agree well with the corresponding calcareous nannofossil zonal assignments. There is some discrepancy in the RP16 and RP15 intervals.

### Site Summary

Radiolarians in varying abundances and states of preservation were recovered from both holes at this site. Poorly preserved radiolarians are characterized by significant fragmentation and dissolution. The sparse upper Oligocene (Sample 165-998A-37X-1, 33–35 cm; 339.73 mbsf) through upper middle Eocene (Sample 165-998B-23R-1, 123–125 cm; 771.33 mbsf) radiolarian assemblages are weakly silicified and show moderate dissolution. A noticeable change in preservation occurs in the upper part of the middle Eocene. Here weakly silicified radiolarian layers alternate with layers of very poorly preserved assemblages. These assemblages containing internal clay casts of radiolarians with remnants of siliceous wall structures are mixed with very rare altered, totally silica-filled radiolarians with a lower refractive index. The lower middle Eocene (Sample 165-998B-26R-3, 63–65 cm; 793.03 mbsf) to lower Eocene (Sample 165-998B-37R-5, 35–37 cm; 901.45 mbsf) part of the section is almost barren of radiolarians, except for the sporadic samples containing many molds of radiolarians. The lower refractive index of these molds is indicative of a structural change in the silica. Chert nodules are present below Core 165-998B-27R.

### Site 999

#### Hole 999B

Hole 999B ( $12^{\circ}44.597'N$ ,  $78^{\circ}44.418'W$ ) was drilled in the Colombian Basin in 2827.9 m of water and represents the best Paleogene radiolarian material recovered on Leg 165. Our samples (Table 3) were taken from between Samples 165-999B-14R-1, 18–20 cm (649.68 mbsf), and 62R-1, 104–106 cm (1065.84 mbsf), which interval, according to nannofossil data, extends from the late Oligocene (CP19b) to the Cretaceous (CC26). Radiolarians in core material above Sample 165-999B-40R-1, 127–129 cm (873.47 mbsf) vary in abundance from few to abundant and in preservation from poor to moderately good, thus allowing for a fairly complete biostratigraphic interpretation. Most of the examined material from below 873.47 mbsf is barren of radiolarians. Only Sample 165-999B-45R-1, 63–65 cm, could be assigned to radiolarian zonal equivalent RP9.

According to the initial reports for this leg (Sigurdsson, Leckie, Acton, et al., 1997), occurrence of a claystone at interval 165-999B-51R-5, 70–135 cm, is thought to reflect a brief interval of decreased carbonate deposition in the latest Paleocene. The timing of this event suggests a correlation with oceanographic and climatic changes that characterize the late Paleocene thermal maximum (LPTM) (Zachos et al., 1993). The effects of the abrupt warming on the radiolarian assemblage could not be documented because the upper Paleocene through lower Eocene interval in Hole 999B is generally barren of radiolarians except for Samples 165-999B-51R-5, 59–61 cm (974.99 mbsf), and 101–102 cm (975.41 mbsf), which straddle the LPTM interval (Table 3). These assemblages contain abundant, extremely poorly preserved radiolarians indicative of the uppermost Paleocene *Bekoma bidartensis* Zone (RP7).

### Site 1001

#### Hole 1001A

Hole 1001A ( $15^{\circ}45.427'N$ ,  $74^{\circ}54.627'N$ ) was drilled on the lower part of the Nicaraguan Rise in 3259.6 m of water. Our samples (Table 4) were taken from between interval 165-1001A-18R-3, 42–44 cm (163.72 mbsf), and 52R-5, 63–65 cm (483.95 mbsf), which, according to nannofossil data, spans a period from the middle Miocene (CN5) to the Cretaceous (CC22), but there is a major unconformity between the middle Miocene and lower Eocene (between Samples 165-1001A-18R-4, 127–129 cm, and 19R-1, 25–27 cm). The Cretaceous part of this sequence, below Sample 165-1001A-37R-6, 110–112 cm (340.95 mbsf), was not examined in the present study.

**Table 1.** Range chart for stratigraphically important radiolarian species, Hole 998A.

	Subepoch	Nanofossil zone	Radiolarian zone	Core, section, interval (cm)	Depth (mbsf)	Abundance	Preservation	No. of slides examined	<i>Artaphornis gracilis</i>	<i>Calocyctes bandica</i>	<i>Calocyctes turris</i>	<i>Calocyctetta (C.) robusta</i>	<i>Carpocanistrum</i> spp.	<i>Cryptocarpium azyx</i>	<i>Cyrtocapsella tetraperata</i>	<i>Dictyopora mongolfieri</i>	<i>Dictyopora piritum</i>	<i>Didymocystis prismatica</i>	<i>Dorcadopsis aenuchus</i>	<i>Dorcadopsis papilio</i>	<i>Dorcadopsis pseudopapilio</i>	<i>Eucyrtidium diaphanes</i>	<i>Lithocyctella angusta</i>	<i>Lithocyctella aristotelis</i> grp.	<i>Lophocystis (C.) pegetrum</i>	<i>Lychnocanomata amphitrite</i>	<i>Lychnocanomata elongata</i>	<i>Thecocys spongococonus</i>	<i>Thecocystis annosa</i>	<i>Thysocystis (P.) lochites</i>	<i>Thysocystis (P.) reticulata</i>	<i>Thysocystis (T.) bromia</i>	<i>Thysocystis (T.) rhizodon</i>	<i>Tristylospyris triceros</i>
early Oligocene	late Oligocene	RP22	CP19b	165-998A-36X-1, 36-38	330.16	C	MG	11																										
				37X-1, 33-35	339.73	R	P	6																										
				38X-1, 36-38	349.36	F	P	3																										
				39X-CC, 27-29	361.64	tr		5																										
				40X-1, 35-37	368.55	VR	P	3																										
				41X-5, 37-39	383.77	VR	M	9																										
				42X-5, 36-38	393.96	R	MG	2																										
				43X-1, 36-38	397.56	F	MG	3																										
				44X-3, 31-32	410.11	R	P	3																										
				45X-1, 89-91	417.29	tr		5																										
late Eocene		RP20	CP19a	46X-1, 36-38	426.36	R	M	5																										
				47X-1, 42-44	436.12	tr		5																										
				48X-1, 107-109	446.37	tr		2																										
				49X-3, 36-38	458.26	B		2																										
				50X-2, 103-105	467.03	R	P	3																										
				52X-3, 30-32	487.00	R	M	3	+																									
				53X-1, 36-38	493.66	R	M	3																										
				54X-1, 20-22	503.10	R	M	3	+																									
				55X-1, 36-38	512.86	R	M	2	+																									
				56X-3, 33-35	525.43	VR	M	9																										
		CP17	CP18	57X-1, 34-36	532.14	R	M	2	R																									
				58X-3, 34-35	544.74	R	M	3	+																									
				59X-5, 34-36	557.44	tr		2																										
				60X-1, 36-38	561.06	R	M	5																										
				61X-1, 35-37	570.65	tr		2																										
				62X-1, 36-37	580.26	tr		3																										
				63X-1, 35-37	589.85	VR	P	3																										
				64X-1, 3-5	599.13	tr		2																										
				65X-1, 57-59	609.27	VF	P	3	F	R									R	R														
				67X-1, 4-6	628.04	VF	G	5	+	+									R	R	+													
		RP18																																

Notes: Radiolarian abundances are shown as C = common, F = few, VF = very few, R = rare, VR = very rare, tr = trace, and B = barren. Radiolarian preservation is shown as G = good, MG = moderately good, M = moderate, and P = poor. Species abundances are shown as A = abundant, F = few, R = rare, + = single specimen, - = searched for but not found, and ? = dubious identification. Hatching indicates uncertainty in placement of zonal boundary. Shaded row indicates barren sample. See text for key to radiolarian zonal codes.

**Table 2.** Range chart for stratigraphically important radiolarian species, Hole 998B.

Subepoch		Radiolarian zone		Nanofossil zone				
		Core, section, interval (cm)	Depth (mbsf)	Abundance	Preservation	No. of slides examined		
early Oligocene	CP17	RP20	165-998B-				<i>Anthocystis</i> sp.	
			1R-1, 38-40	558.68	VR	M	<i>Anthocystis petrushetskayae</i>	
			1R-3, 38-40	561.68	VR	M	<i>Antiphormis gracilis</i>	
			1R-5, 33-35	564.63	F	M	<i>Calocyclus bandica</i>	
			2R-1, 34-36	568.24	tr	F	<i>Calocyclus hispida</i>	
	CP16c		2R-3, 33-35	571.23	F	M	<i>Calocyclus turris</i>	
			2R-5, 20-22	574.10	R	M		
			3R-1, 17-19	577.67	VR	M		
			3R-3, 23-25	580.73	tr	M		
			3R-5, 40-42	583.90	B	P		
late Eocene	CP15	RP18	4R-1, 36-38	587.46	tr	P		
			4R-3, 36-37	590.46	tr	P		
			4R-5, 34-35	593.44	R	P		
			5R-1, 50-52	597.30	tr	P		
			5R-3, 41-43	600.21	tr	P		
	?RP17		5R-5, 25-27	603.05	VR	P		
			6R-1, 21-23	606.51	R	P		
			6R-3, 26-28	609.56	C	MG		
			6R-5, 26-28	612.56	tr	F		
			7R-1, 30-32	616.30	F	MG		
middle Eocene	CP14b	?RP17/CP18 I. EOC	7R-3, 13-15	619.13	R	P		
			7R-5, 4-6	622.04	R	P		
			8R-1, 17-19	625.77	F	M		
			8R-3, 22-24	628.82	VF	M		
			8R-5, 31-33	631.91	F	M		
	?RP17/CP18 II. EOC		9R-1, 35-37	635.55	R	M		
			9R-3, 36-38	638.56	tr	P		
			9R-5, 37-39	641.57	R	P		
			10R-1, 36-38	645.16	R	M		
			10R-3, 36-38	648.16	tr	P		
middle Miocene	CP14a	RP16	10R-5, 36-38	651.16	tr	P		
			11R-1, 45-47	654.95	VR	MG		
			11R-3, 32-34	657.82	VR	MG		
			12R-1, 34-36	664.44	R	M		
			12R-3, 39-41	667.49	VR	M		
	?RP15/CP16		13R-1, 34-36	674.14	tr	P		
			13R-3, 40-42	677.20	R	M		
			13R-5, 33-35	680.13	R	M		
			14R-1, 29-31	683.79	F	M		
			14R-3, 32-34	686.82	F	G		
late Miocene	CP14a	?RP15/CP16	15R-1, 37-39	693.47	F	M		
			15R-3, 34-36	696.44	F	M		
			15R-5, 21-23	698.51	R	M		
			16R-1, 49-51	703.19	F	M		
			16R-3, 19-21	705.89	F	M		
	?RP13/CP14		17R-1, 81-83	713.11	tr	P		
			17R-3, 37-39	715.67	VR	M		
			18R-1, 27-29	722.27	tr	P		
			18R-3, 53-55	725.53	tr	P		
			18R-5, 70-73	728.70	tr	P		
Pliocene	CP14a	RP15/CP16	19R-1, 41-43	732.01	tr	P		
			19R-3, 41-43	735.01	C	P		
			19R-5, 31-33	737.91	tr	P		
			20R-1, 41-43	741.61	C	MG		
			20R-3, 38-39	744.58	C	P		
	?RP13/CP14		21R-1, 37-39	751.17	F	MG		
			21R-3, 35-37	754.15	F	P		
					R			

**Table 2 (continued).**

Subepoch		Radiolarian zone		Core, section, interval (cm)		Depth (mbsf)		Abundance		Preservation		Nanofossil zone		
middle Eocene	CP13c	?RP13/RP14 ? RP13	21R-5, 96-98	757.76	A	MG	5	No. of slides examined						
			22R-1, 36-38	760.86	A	P	5	<i>Anthocyrtoma</i> sp.						
			22R-3, 35-37	763.85	A	P-VP	5	<i>Artiphormis gracilis</i>						
			22R-5, 35-37	766.85	C	MG	6	<i>Calocyclas bandycza</i>						
			23R-1, 123-125	771.33	A	M	2	<i>Calocyclas hispida</i>						
	CP13b	?RP12 ? RP12	23R-3, 39-41	773.49	C	VP	5	<i>Calocyclas turris</i>						
			23R-5, 45-47	776.21	A	P	4	<i>Calocyctoma ampla</i>						
			24R-1, 35-37	777.45	A	VP	4	<i>Centrobrotyx pernitshevskayae</i>						
			25R-3, 28-30	783.08	A	VP	4	<i>Ceratospirys articulata</i>						
			25R-5, 46-48	786.26	B	P-M	2	<i>Cryptocarpium azyx</i>						
early Eocene	CP13a	CP12	26R-1, 34-36	789.74	A	P	2	<i>Dicytophimus cranicula</i>						
			26R-3, 63-65	793.03	B	P	2	<i>Dicytopyrora armadillo</i>						
			26R-5, 33-35	795.73	B	P	2	<i>Dicytopyrora mongolfieri</i>						
			27R-1, 35-37	799.25	B	P	2	<i>Dicytopyrora pirum</i>						
			27R-3, 35-37	802.25	B	P	2	<i>Eusyringium fistuliferum</i>						
	CP11	?RP8	27R-5, 36-38	805.26	B	P	2	<i>Lithocyrtis vespertilio</i>						
			28R-1, 36-37	808.86	B	P	2	<i>Lithocyctia angusta</i>						
			28R-3, 36-38	811.86	B	P	2	<i>Lithocyctia aristotelia</i> grp.						
			28R-5, 50-52	815.00	B	P	2	<i>Lithocyctia ocellus</i>						
			29R-1, 25-27	818.45	B	P	2	<i>Lophocyrtis (C.) milowi</i>						
CP10	CP12	31R-1, 28-30	29R-3, 25-27	821.43	tr	P	2	<i>Lycchnocanomma amphitrite</i>						
			29R-5, 28-30	824.46	B	VP	2	<i>Lycchnocanomma babylonis</i> grp.						
			30R-1, 32-34	828.12	B	VP	2	<i>Lycchnocanomma bellum</i>						
			30R-3, 24-26	831.04	B	VP	2	<i>Phormocystis striata striata</i>						
			30R-5, 12-14	833.92	B	VP	2	<i>Podocystis (L.) chalara</i>						
	CP11	31R-1, 28-30	31R-1, 28-30	837.78	tr	P	2	<i>Podocystis (L.) fasciolata</i>						
			31R-3, 29-31	840.79	R	VP	2	<i>Podocystis (L.) goetheana</i>						
			31R-5, 45-47	843.93	C	VP	4	<i>Podocystis (L.) mira</i>						
			32R-1, 36-38	847.46	B	VP	2	<i>Podocystis (L.) simuosa</i>						
			32R-3, 2-4	850.07	B	VP	2	<i>Podocystis (L.) trachodes</i>						
CP10	CP12	32R-5, 41-43	32R-5, 41-43	853.46	B	VP	2	<i>Podocystis (P.) ampla</i>						
			33R-1, 39-41	857.09	B	VP	2	<i>Podocystis (P.) papalis</i>						
			33R-3, 39-41	860.09	tr	VP	2	<i>Rhopalocanum ornatum</i>						
			33R-5, 36-38	863.02	B	VP	2	<i>Sethocystis triconicus</i>						
			34R-1, 35-37	866.65	C	VP	2	<i>Spongatractus pachystylus</i>						
	CP11	34R-3, 36-38	34R-3, 36-38	869.66	B	VP	2	<i>Thecocystis anaprapha</i>						
			34R-5, 36-38	872.66	B	VP	2	<i>Thecocystis conica</i>						
			35R-1, 31-33	876.21	B	VP	4	<i>Thecocyste cryocephala</i>						
			35R-3, 31-33	879.21	B	VP	4	<i>Thecocystis fibrosa</i>						
			35R-5, 31-33	882.21	F	VP	2	<i>Thaumatocyrtis tenuis</i>						
CP10	CP12	36R-1, 42-44	36R-1, 35-37	885.92	B	VP	2	<i>Thrysoecystis (P.) tensa</i>						
			36R-3, 25-27	888.75	B	VP	2	<i>Thrysoecystis (P.) tetricantha</i>						
			36R-5, 21-23	891.71	B	VP	2	<i>Thrysoecystis (T.) bronii</i>						
			37R-1, 13-15	895.23	B	VP	2	<i>Thrysoecystis (T.) rhizodon</i>						
			37R-3, 6-8	898.16	A	VP	3	<i>Tritylosiopsis tricornis</i>						
	CP11	37R-5, 35-37	37R-5, 35-37	901.45	B	VP	2							

Notes: Radiolarian abundances are shown as A = abundant, C = common, F = few, VF = very few, R = rare, VR = very rare, tr = trace, and B = barren. Radiolarian preservation is shown as G = good, MG = moderately good, M = moderate, and P = poor. Species abundances are shown as C = common, F = few, MR = moderately rare, R = rare, + = single specimen, - = searched for but not found, ? = dubious identification, and X = present in undetermined quantities. Radiolarian zones determined only for isolated samples. Shaded rows indicates barren samples. See text for key to radiolarian zonal codes.

**Table 3.** Range chart for stratigraphically important radiolarian species, Hole 999B.

Table 3 (continued).

Subepoch		late Oligocene		early Oligocene		late Eocene		middle Eocene		late Oligocene		Subepoch		Nannofoossil zone		Core, section, interval (cm)	Depth (mbsf)	Abundance	Preservation	No. of slides examined					
		CP19b	RP21	CP19a	RP20	CP18	RP20	CP17	RP19	CP16a/b	RP19	CP15	RP18	CP15	RP17	CP14b	RP16	CP14a	RP15	CP14a	RP14	CP13c	RP13	CP13b	RP13
165-999B-																									
14R-1, 18-20		649.68	R, VR	F, VR	VP, MG	C, VR	VP, MG																		
14R-3, 31-33		651.82																							
14R-5, 26-28		654.77																							
15R-1, 24-26		659.34	C, R	V, P, M																					
15R-3, 23-25		662.33	A, R	V, P, G																					
16R-1, 20-22		669.00	A, R	V, P, G																					
16R-3, 21-23		670.80	C	V, P																					
16R-5, 16-18		673.75	F	M																					
19R-1, 23-25		682.13	A, VR	V, P, M																					
20R-1, 18-20		685.08	C	V, P																					
21R-1, 19-21		688.09	VR	M																					
21R-5, 20-22		694.10	F	V, P																					
22R-1, 17-19		697.77	B																						
22R-3, 17-19		700.77	C	VP																					
23R-1, 22-24		707.42	A, VR	VP, M																					
23R-3, 25-27		710.45	F	V, P																					
23R-5, 23-25		713.43	tr																						
24R-3, 23-25		719.93	A	P-M																					
24R-5, 22-24		722.92	A	P																					
25R-1, 31-33		726.91	A	VP																					
25R-3, 20-22		729.20	F	V, P																					
25R-5, 21-23		731.41	A	P																					
25R-7, 8-10		734.28	F	VP																					
26R-1, 12-14		736.42	C	V, P																					
26R-3, 23-25		739.53	F, VR	V, P, G																					
26R-5, 13-15		742.43	A	P																					
27R-1, 19-21		746.19	A	P-G																					
27R-3, 13-15		749.11	A	VP																					
27R-5, 19-21		752.17	A	VP																					
28R-1, 0-2		755.7	A	MG																					
28R-3, 14-16		758.84	A	M																					
28R-5, 2-4		761.72	A	VP																					
29R-1, 40-42		765.80	A	MG																					
29R-3, 14-16		768.54	F	VP																					
29R-5, 72-74		772.12	A	MG																					
30R-1, 57-59		775.67	F	MG																					
30R-3, 72-73		778.82	A	MG																					
31R-1, 131-133		786.21	C	VP																					
31R-3, 12-14		788.02	A	M																					
31R-5, 62-64		790.62	C	VP																					
32R-1, 40-42		795.20	A	M																					
33R-1, 78-80		805.48	A	M																					
33R-3, 55-57		808.25	C	VP																					
33R-5, 54-56		811.24	A	M																					
34R-1, 55-57		815.05	A	M																					
34R-3, 53-55		818.03	A	M-P																					
34R-5, 15-17		820.65	A	P																					
35R-1, 73-75		824.83	A	M-G																					
35R-3, 18-20		827.28	A	M-P																					
36R-2, 120-122		836.40	A	MG																					
36R-4, 7-9		838.27	A	MG																					
37R-1, 76-78		844.06	C	VP																					
37R-3, 143-145		847.73	A	VP																					
38R-1, 10-12		853.00	C	VP																					
38R-3, 120-122		857.10	B																						
39R-1, 135-137		863.95	tr																						

**Table 3 (continued).**

Table 3 (continued).

late Paleocene		early Eocene		middle Eocene		Subepoch		Radiolarian zone		Nanofossil zone				
early Paleocene	CP2/3	CP4	CP5	CP6/7	CP9	CP10/11	RP9	CP12/13a						
									Core, section, interval (cm)	Depth (mbsf)	Abundance			
												Preservation		
									No. of slides examined					
									<i>Phormocyris cubensis</i>					
									<i>Phormocyris striata exquisita</i>					
									<i>Phormocyris striata striata</i>					
									<i>Phormocyris turgida</i>					
									<i>Podocyris (L.) chalara</i>					
									<i>Podocyris (L.) fasciolata</i>					
									<i>Podocyris (L.) goethiana</i>					
									<i>Podocyris (L.) mitra</i>					
									<i>Podocyris (L.) sinuosa</i>					
									<i>Podocyris (L.) trachodes</i>					
									<i>Podocyris (P.) ampla</i>					
									<i>Podocyris (P.) diamesa</i>					
									<i>Podocyris (P.) papalis</i>					
									<i>Rhabdolithis pipa</i>					
									<i>Rhopalocanium ornatum</i>					
									<i>Sethocyris triconicus</i>					
									<i>Spongarractus pachystylus</i>					
									<i>Stichomitra granulata</i>					
									<i>Thecoctys analasta</i>					
									<i>Thecoctyle cryptocephala</i>					
									<i>Thecoctyllissa alpha</i>					
									<i>Thecoctyllissa ficus</i>					
									<i>Thecoctyllissa annosa</i>					
									<i>Thecoviridis tuberosa</i>					
									<i>Thysocystis (P.) lochites</i>					
									<i>Thysocystis (P.) tetricantha</i>					
									<i>Thysocystis (P.) triacantha</i>					
									<i>Thysocystis (T.) bromia</i>					
									<i>Thysocystis (T.) hirsuta</i>					
									<i>Thysocystis (T.) rhizodon</i>					
									<i>Trityllospyris tricuspidata</i>					
									<i>Trityllospyris tricuspidata</i>					

**Table 3 (continued).**

		Subepoch	Nanofossil zone	Radiolarian zone	Core, section, interval (cm)	Depth (mbsf)	Abundance	Preservation	No. of slides examined
Cret.	CC26				61R-3, 80-82 61R-5, 79-81 62R-1, 104-106	1058.90 1061.89 1065.84	B VR B	G	2 4 2
									<i>Amphicraspedium murrayanum</i>
								X	<i>Anthocyrtina</i> sp.
									<i>Artoophormis gracilis</i>
									<i>Buryella clinata</i>
									<i>Buryella</i> spp.
									<i>Calocyclas bandycra</i>
									<i>Calocyclas hispida</i>
									<i>Calocyclas turris</i>
									<i>Calocyctoma ampulla</i>
									<i>Carpacanistrum</i> spp.
									<i>Centroborys gravida</i>
									<i>Centroborys petrusheskayae</i>
									<i>Cryptocarpium aegyptium</i>
									<i>Cryptocarpium ornatum</i>
									<i>Dicytophora craticula</i>
									<i>Dicytophora amphora</i> grp.
									<i>Dicytophora armadillo</i>
									<i>Dicytophora mongolfieri</i>
									<i>Dicytophora pirim</i>
									<i>Dorcadospyris ateuchus</i>
									<i>Dorcadospyris papilio</i>
									<i>Eucyrtidium diaphanes</i>
									<i>Eusyringium fistuligerum</i>
									<i>Eusyringium lagena</i>
									<i>Lamponium fab. chaunothorax</i>
									<i>Lithochytris vesperitillo</i>
									<i>Lithocyclia angusta</i>
									<i>Lithocyclia aristotelis</i> grp.
									<i>Lithocyclia ocellus</i> grp.
									<i>Lophocystis biaurita</i>
									<i>Lophocystis (C.)</i> spp.
									<i>Lychnocanoma amphitrite</i>
									<i>Lychnocanoma balyonis</i> grp.
									<i>Lychnocanoma bajunensis</i>

Notes: Radiolarian abundances are shown as A = abundant, C = common, F = few, VF = very few, R = rare, VR = very rare, tr = trace, and B = barren. Radiolarian preservation is shown as G = good, MG = moderately good, M = moderate, P = poor, and VP = very poor. Preservations shown as M-G, for example, indicate a range of preservation states. In some cases the abundance of two different preservation states is noted as, for example, R, VR in the abundance column and VP, MG in the preservation column indicating the presence of rare very poorly preserved forms and very rare moderately well-preserved forms. Species abundances are shown as C = common, F = few, VF = very few, MR = moderately rare, R = rare, - = searched for but not found, ? = dubious identification, and X = present in undetermined quantities. Hatching indicates uncertainty in placement of zonal boundary. Shaded rows indicate barren samples. See text for key to radiolarian zonal codes.

**Table 3 (continued).**

		Subepoch	Nanofossil zone	Radiolarian zone	Core, section, interval (cm)	Depth (mbsf)	Abundance	Preservation	No. of slides examined
Cret.	CC26				61R-5, 79-81 61R-3, 80-82 62R-1, 104-106	1061.89 1058.90 1065.84	VR B B	G	4 2
									<i>Phormocytis cubensis</i>
								X	<i>Phormocytis striata exquisita</i>
									<i>Phormocytis striata striata</i>
									<i>Phormocytis turgida</i>
									<i>Podocyrtis (L.) chalara</i>
									<i>Podocyrtis (L.) fasciolata</i>
									<i>Podocyrtis (L.) goetheana</i>
									<i>Podocyrtis (L.) mitra</i>
									<i>Podocyrtis (L.) sinuosa</i>
									<i>Podocyrtis (L.) trachodes</i>
									<i>Podocyrtis (P.) ampla</i>
									<i>Podocyrtis (P.) diamesa</i>
									<i>Podocyrtis (P.) papalis</i>
									<i>Rhabdolithis pipa</i>
									<i>Rhopalocanium ornatum</i>
									<i>Sethoclytis triconicus</i>
									<i>Spongulariacus pachystylus</i>
									<i>Stichomitra granulata</i>
									<i>Thecoctys anacelsis</i>
									<i>Thecoctyle crypoccephala</i>
									<i>Thecoctys alpha</i>
									<i>Thecoctys ficus</i>
									<i>Thecoctys annosa</i>
									<i>Thecoctys tuberosa</i>
									<i>Thysocystis (P.) lochites</i>
									<i>Thysocystis (P.) tereticantha</i>
									<i>Thysocystis (P.) triacantha</i>
									<i>Thysocystis (T.) bromia</i>
									<i>Thysocystis (T.) hirsuta</i>
									<i>Thysocystis (T.) rhizodon</i>
									<i>Tritylospirifer triceratops</i>

**Table 4.** Range chart for stratigraphically important radiolarian species, Hole 1001A.

Notes: Radiolarian abundances are shown as A = abundant, C = common, F = few, R = rare, VR = very rare, tr = trace, and B = barren. Radiolarian preservation is shown as G = good, MG = moderately good, M = moderate, and VP = very poor. A, R in the abundance column and VP, G in the preservation column indicate the presence of abundant very poorly preserved forms and rare well-preserved forms in the same sample. Species abundances are shown as C = common, F = few, VF = very few, MR = moderately rare, R = rare, + = single specimen, - = searched for but not found, ? = dubious identification, and X = present in undetermined quantities. Radiolarian zones determined only for isolated samples. Shaded rows indicate barren samples. See text for key to radiolarian zonal codes.

### Hole 1001B

Hole 1001B replicated, in part, Hole 1001A, and our samples were taken from the Paleocene (calcareous nannofossil Zones CP8 to CP4) part of the hole, in Samples 165-1001B-6R-1, 69–71 cm (235.99 mbsf) to 14R-6, 20–22 cm (319.90 mbsf). Preservation in all our samples was poor to extremely poor with evidence of recrystallization and infilling. Sample 165-1001B-6R-1, 69–71 cm, contains abundant, but poorly to moderately well-preserved radiolarians and can be placed in radiolarian zonal equivalent RP7. Radiolarians in Samples 165-1001B-7R-1, 3–5 cm, to 12R-1, 28–30 cm, range in abundance from barren to very rare and are all poorly preserved. Between Samples 165-1001B-12R-3, 58–60 cm, and 14R-6, 20–22 cm, radiolarians are more abundant (few to common), but, once again, the preservation is very poor. We were, however, able to determine that Samples 165-1001B-6R-1, 69–71 cm, to 12R-3, 58–60 cm, lie within radiolarian zonal equivalent RP7 and samples below this level belong to radiolarian zonal equivalent RP6.

### Site Summary

The Paleocene/Eocene boundary could not be identified at this site by either calcareous nannofossil or radiolarian biostratigraphies. Deteriorating preservation and extremely impoverished radiolarian faunas prevent confident subdivision of the upper Paleocene interval. However, it is noteworthy that the 56- to 75-cm-thick clayey interval that is characterized by reduced carbonate content and multiple ash layers was cored in two holes at Site 1001 (intervals 165-1001A-27R-2, 0–56 cm, and 165-1001B-6R-3, 0–75 cm). Preliminary calcareous biostratigraphy (Sigurdsson, Leckie, Acton, et al., 1997) suggests that this interval correlates with the widespread oceanographic changes associated with the LPTM (Zachos et al., 1993). As in Hole 999B, where this interval was also recovered, radiolarian abundance increases markedly (Sample 165-1001A-27R-1, 108–110 cm) in this interval relative to samples immediately above and below it. Zeolites are particularly abundant in the radiolarian-barren samples (Samples 165-1001A-27R-1, 46–48 cm; 237.66 mbsf, and 27R-3, 48–50 cm; 240.68 mbsf) surrounding the LPTM interval. Sample 165-1001A-27R-1, 46–48 cm (237.66 mbsf), contains, in addition to the zeolites, altered glass shards with abundant plagioclase phenocrysts and very common large hornblende crystals (P. Worstell, pers. comm., 1998). In the LPTM interval, the assemblage is composed of abundant, poorly preserved radiolarians together with rare, well-preserved taxa representing the *Bekoma bidartensis* Zone (RP7). At this time, it is not possible to determine if the sparse assemblages above and below the LPTM are the result of oceanographic changes associated with the LPTM or the result of dissolution.

Despite the generally poor faunal assemblage found in Hole 1001B, we think that the improvement in radiolarian preservation in Sample 165-1001B-6R-1, 69–71 cm, which contains abundant, poor to moderately well-preserved radiolarians, may also be associated with the oceanographic events related to the LPTM interval. Our samples below this level are essentially barren, as was the case below the LPTM in Holes 999B and 1001A, but we do not have the corresponding samples from above this level.

### CONCLUSIONS

In general, our Leg 165 samples were highly lithified and, as a result, required lengthy and repetitive cleanings. In the majority of our samples we found that radiolarians are either extremely rare, represented by dissolved fragments, or masked by clay and/or ash in such a way that species identification was often difficult and required examination of numerous microscope slides. It was possible, however,

to construct at least partial stratigraphies for each of the three sites examined.

It is difficult to envision sufficiently large variations in productivity within the restricted Caribbean environment to account for the marked differences between silica preservation at Sites 998, 999, and 1001 and other Caribbean sites, and certainly productivity variation cannot account for the range of preservation within a given sample. Most of the radiolarians originally deposited in the material were probably not preserved, not even as molds, but were destroyed in situ by dissolution following burial. Silica released by dissolution was subsequently reprecipitated inorganically to form a significant portion of the matrix and constitutes the principal lithifying agent.

Previous investigators (Reynolds, 1966, 1970; Heron, 1969; Gibson and Towe, 1971) concluded that the presence of silica-rich opaline claystones in Paleogene rocks of the Atlantic and Gulf Coast Plain are the result of the deposition of volcanic materials in shallow coastal environments. Evidence from scanning electron microscopy and petrographic studies of opaline claystones containing numerous molds and tests of siliceous microfossils suggested to them that the source of silica for these deposits would be biogenous rather than volcanic, although volcanic ashfalls may be considered as ultimate silica sources (Wise and Weaver, 1973). Paleontological and stratigraphic evidence (Riedel and Sanfilippo, 1970, 1973; Sanfilippo and Riedel, 1973; Foreman, 1973; Maurrasse, 1979) also suggest that the production of siliceous planktonic organisms and geological conditions favored deposition of siliceous sediments in the Caribbean Sea during the Paleogene and that their absence in the sediments is caused by dissolution after burial.

An interval associated with the LPTM was observed by the shipboard scientists in Holes 999B, 1001A, and 1001B. In our samples from these holes we have observed a marked increase in radiolarian abundance and an improvement in their preservation during these intervals relative to assemblages above and below the interval. Samples from within the LPTM interval belong to the upper part of the *Bekoma bidartensis* Zone (RP7), which spans the Paleocene/Eocene boundary.

### ACKNOWLEDGMENTS

We would like to thank ODP for allowing us to obtain Leg 165 samples and members of the shipboard party for actual sample collection. In particular, we would like to thank Mark Leckie, Tim Brauner, and Ellen Thomas for their support and interest during our investigations. The manuscript benefited from reviews by Ted Moore and Chris Hollis. This study was supported by Grant USSSP-204 from the U.S. Science Support Program to the senior author.

### REFERENCES

- Borisenko, N.N., 1958. Radiolyari paleotsena zapadnoi Kubani (Paleocene radiolaria of Western Kuban). *Tr. Vses. Nauchno-Issled. Inst. Krasnodarskii Filial*, 17:81–100.
- Brandt, R., 1935. Die Mikropalaeontologie des Heiligenhafener, Kieseltones (Ober-Eozan) Radiolarien, Systematik. *In* Wetzel, E.O. (Ed.), *Jahresbericht des Niedersächsischen Geologischen Vereins*, 27:48–59.
- Cande, S.C., and Kent, D.V., 1995. Revised calibration of the geomagnetic polarity timescale for the Late Cretaceous and Cenozoic. *J. Geophys. Res.*, 100:6093–6095.
- Carnevale, P., 1908. Radiolarie e silicoflagellati di Bergonzano (Reggio Emilia). *Veneto Sci. Lett. Arti Mem.*, 28:1–46.
- Cita, M.B., Nigrini, C., and Gartner, S., 1970. Biostratigraphy. *In* Peterson, M.N.A., et al., *Init. Repts. DSDP*, 2: Washington (U.S. Govt. Printing Office), 391–411.
- Clark, B.L., and Campbell, A.S., 1942. Eocene radiolarian faunas from the Mt. Diablo area, California. *Spec. Pap.—Geol. Soc. Am.*, 39:1–112.

- Dumitrica, P., 1973. Paleocene radiolaria, DSDP Leg 21. In Burns, R.E., Andrews, J.E., et al., *Init. Repts. DSDP*, 21: Washington (U.S. Govt. Printing Office), 787–817.
- Ehrenberg, C.G., 1847. Über die mikroskopischen kieselschaligen Polycystinen als mächtige Gebirgsmasse von Barbados und über das Verhältniss deraus mehr als 300 neuen Arten bestehenden ganz eigenthümlichen Formengruppe jener Felssmasse zu den jetzt lebenden Thieren und zur Kreidebildung. Eine neue Anregung zur Erforschung des Erdlebens. *K. Preuss. Akad. Wiss. Berlin, Bericht*, Jahre 1847:40–60.
- , 1854. *Mikrogeologie: Das Erden und Felsen schaffende Wirken des unsichtbar kleines selbständigen Lebens auf der Erde*: Leipzig (Leopold Voss).
- , 1873. Grössere Felsproben des Polycystinen-Mergels von Barbados mit weiteren Erläuterungen. *K. Preuss. Akad. Wiss. Berlin, Monatsberichte*, Jahre 1873:213–263.
- , 1875. Fortsetzung der mikrogeologischen Studien als Gesammt-Uebersicht der mikroskopischen Paläontologie gleichartig analysirter Gebirgsarten der Erde, mit specieller Rücksicht auf den Polycystinen-Mergel von Barbados. *Abh. K. Akad. Wiss. Berlin*, Jahre 1875:1–225.
- Florez Abin, E., 1983. Radiolarios de algunas formaciones del Cretacico Paleogeno Inferior de Cuba occidental. *Cienc. Tierra Esp.*, 7:1–36.
- Foreman, H.P., 1973. Radiolaria of Leg 10 with systematics and ranges for the families Amphipyndacidae, Artostrobiidae, and Theoperidae. In Worzel, J.L., Bryant, W., et al., *Init. Repts. DSDP*, 10: Washington (U.S. Govt. Printing Office), 407–474.
- , 1975. Radiolaria from the North Pacific, Deep Sea Drilling Project, Leg 32. In Larson, R.L., Moberly, R., et al., *Init. Repts. DSDP*, 32: Washington (U.S. Govt. Printing Office), 579–676.
- Gibson, T.G., and Towe, K.M., 1971. Eocene volcanism and the origin of Horizon A. *Science*, 172:152–154.
- Goll, R.M., 1969. Classification and phylogeny of Cenozoic Trissocyklidae (Radiolaria) in the Pacific and Caribbean basins, Part II. *J. Paleontol.*, 43:322–339.
- , 1972. Leg 9 synthesis, radiolaria. In Hays, J.D., et al., *Init. Repts. DSDP*, 9: Washington (U.S. Govt. Printing Office), 947–1058.
- Haeckel, E., 1887. Report on the Radiolaria collected by H.M.S. *Challenger* during the years 1873–1876. *Rep. Sci. Results Voy. H.M.S. Challenger, 1873–1876, Zool.*, 18:1–1803.
- Heron, S.D., 1969. Mineralogy of the Black Mingo mudrocks. *S.C. State Develop. Bd., Div. Geol., Geol. Notes*, 13:2741.
- Hollis, C.J., 1993. Latest Cretaceous to Late Paleocene radiolarian biostratigraphy: a new zonation from the New Zealand region. *Mar. Micropaleontol.*, 21:295–327.
- Kling, S.A., 1971. Radiolaria: Leg 6 of the Deep Sea Drilling Project. In Fischer, A.G., Heezen, B.C., et al., *Init. Repts. DSDP*, 6: Washington (U.S. Govt. Printing Office), 1069–1117.
- Kozlova, G.E., and Gorbovets, A.N., 1966. Radiolyarii verkhneemelyovkh i verkhneotsenovykh otlozhennii Zapadno-Sibirskoi Nizmennosti [Radiolaria of the Upper Cretaceous and upper Eocene of the west Siberian Lowland]. *Tr. Vses. Neft. Nauchno-Issled. Geologorazved. Inst.*, 248:1–159.
- Krasheninnikov, V.A., 1960. Nektorye Radiolyarii Nizhnego i Srednego Eot-sens Zapadnogo Predkavkaza (Some radiolarians of the Lower and middle Eocene of the West Caucasus). *Min. Geol. Okhr. Nedr SSSR, Vses. Nauchno-Issled. Geol. Neft. Inst.*, 16:271–308.
- Ling, H.Y., 1975. Radiolaria: Leg 31 of the Deep Sea Drilling Project. In Karig, D.E., Ingle, J.C., Jr., et al., *Init. Repts. DSDP*, 31: Washington (U.S. Govt. Printing Office), 703–761.
- Mato, C.Y., and Theyer, F., 1980. *Lychnocanoma bandyca* n. sp., a new stratigraphically important late Eocene radiolarian. In Sliter, W.V. (Ed.), *Studies in Marine Micropaleontology and Paleoecology: A Memorial Volume to Orville L. Bandy*. Spec. Publ. Cushman Found. Foram. Res., 19:225–229.
- Maurrasse, F.J.-M.R., 1979. Cenozoic radiolarian paleobiogeography: implications concerning plate tectonics and climatic cycles. *Palaeogeogr., Palaeoclimatol., Palaeoecol.*, 26:253–289.
- Moore, T., 1971. Radiolaria. In Tracey, J.I., Jr., Sutton, G.H., et al., *Init. Repts. DSDP*, 8: Washington (U.S. Govt. Printing Office), 727–775.
- Nigrini, C., 1974. Cenozoic Radiolaria from the Arabian Sea, DSDP Leg 23. In Davies, T.A., Luyendyk, B.P., et al., *Init. Repts. DSDP*, 26: Washington (U.S. Govt. Printing Office), 1051–1121.
- , 1977. Tropical Cenozoic Artostrobiidae (Radiolaria). *Micropaleontology*, 23:241–269.
- Nishimura, A., 1992. Paleocene radiolarian biostratigraphy in the northwest Atlantic at Site 384, Leg 43, of the Deep Sea Drilling Project. *Micropaleontology*, 38:317–362.
- Petrushevskaya, M.G., 1977. Novye vidy radiolyarii otryada Nassellaria (New species of the radiolarians of the order Nassellaria). In *Issledovaniya fauny moreii: novye vidy i rody morskikh bespozvonochnykh. Sbornik nauchnykh rabot (Exploration of the Fauna of the Seas: New Species and Genera of Marine Invertebrates)*. Zool. Z., Akad. Nauk SSSR, 10–19.
- Petrushevskaya, M.G., and Kozlova, G.E., 1972. Radiolaria, Leg 14, Deep Sea Drilling Project. In Hayes, D.E., Pimm, A.C., et al., *Init. Repts. DSDP*, 14: Washington (U.S. Govt. Printing Office), 495–648.
- Renz, G.W., 1984. Cenozoic radiolarians from the Barbados Ridge, Lesser Antilles subduction complex, Deep Sea Drilling Project Leg 78A. In Biju-Duval, B., Moore, J.C., et al., *Init. Repts. DSDP*, 78: Washington (U.S. Govt. Printing Office), 447–462.
- Reynolds, W.R., 1966. Stratigraphy and genesis of clay mineral and zeolite strata in the lower Tertiary of Alabama. In Copeland, C. (Ed.), *Facies Changes in the Alabama Tertiary*. Ala. Geol. Soc. Guidebook, 26–37.
- , 1970. Mineralogy and stratigraphy of lower Tertiary clays and claystones of Alabama. *J. Sediment. Petrol.*, 40:829–838.
- Riedel, W.R., 1959. Oligocene and Lower Miocene Radiolaria in tropical Pacific sediments. *Micropaleontology*, 5:285–302.
- Riedel, W.R., and Sanfilippo, A., 1970. Radiolaria, Leg 4, Deep Sea Drilling Project. In Bader, R.G., Gerard, R.D., et al., *Init. Repts. DSDP*, 4: Washington (U.S. Govt. Printing Office), 503–575.
- , 1971. Cenozoic Radiolaria from the western tropical Pacific, Leg 7. In Winterer, E.L., Riedel, W.R., et al., *Init. Repts. DSDP*, 7 (Pt. 2): Washington (U.S. Govt. Printing Office), 1529–1672.
- , 1973. Cenozoic Radiolaria from the Caribbean, Deep Sea Drilling Project, Leg 15. In Edgar, N.T., Saunders, J.B., et al., *Init. Repts. DSDP*, 15: Washington (U.S. Govt. Printing Office), 705–751.
- , 1978. Stratigraphy and evolution of tropical Cenozoic radiolarians. *Micropaleontology*, 24:61–96.
- Sanfilippo, A., 1990. Origin of the subgenera *Cyclampterium*, *Paralampterium* and *Sciadiopeplus* from *Lophocyrtis* (*Lophocyrtis*) (Radiolaria, Theoperidae). *Mar. Micropaleontol.*, 15:287–312.
- Sanfilippo, A., Burckle, L.H., Martini, E., and Riedel, W.R., 1973. Radiolarians, diatoms, silicoflagellates and calcareous nanofossils in the Mediterranean Neogene. *Micropaleontology*, 19:209–234.
- Sanfilippo, A., and Hull, D.M., in press. Upper Paleocene-Lower Eocene radiolarian biostratigraphy of the San Francisco de Paula section, western Cuba: regional and global comparisons. *Micropaleontology*.
- Sanfilippo, A., and Nigrini, C., 1995. Radiolarian stratigraphy across the Oligocene/Miocene transition. *Mar. Micropaleontol.*, 24:239–285.
- , 1998a. Code numbers for Cenozoic low latitude radiolarian biostratigraphic zones and GPTS conversion tables. *Mar. Micropaleontol.*, 33:109–156.
- , 1998b. Radiolarian stratigraphy at the Paleocene/Eocene boundary. In Lucas, S., Berggren, W., and Aubry, M.-P. (Eds.), *The Paleocene/Eocene Boundary*: New York (Columbia Univ. Press), IGCP Proj. 308, 244–276.
- Sanfilippo, A., and Riedel, W.R., 1970. Post-Eocene “closed” theoperid radiolarians. *Micropaleontology*, 16:446–462.
- , 1973. Cenozoic Radiolaria (exclusive of theoperids, artostrobiids and amphipyndacids) from the Gulf of Mexico, Deep Sea Drilling Project Leg 10. In Worzel, J.L., Bryant, W., et al., *Init. Repts. DSDP*, 10: Washington (U.S. Govt. Printing Office), 475–611.
- , 1980. A revised generic and suprageneric classification of the Artiscinae (Radiolaria). *J. Paleontol.*, 54:1008–1011.
- , 1982. Revision of the radiolarian genera *Theocotyle*, *Theocotylissa*, and *Thrysocyrtis*. *Micropaleontology*, 28:170–188.
- , 1992. The origin and evolution of Pterocorythidae (Radiolaria): a Cenozoic phylogenetic study. *Micropaleontology*, 38:1–36.
- Sanfilippo, A., Westberg-Smith, M.J., and Riedel, W.R., 1985. Cenozoic radiolaria. In Bolli, H.M., Saunders, J.B., and Perch-Nielsen, K. (Eds.), *Plankton Stratigraphy*: Cambridge (Cambridge Univ. Press), 631–712.
- Saunders, J.B., Bernoulli, D., Mueller-Metz, E., Oberhänsli, H., Perch-Nielsen, K., Riedel, W.R., Sanfilippo, A., and Torrini, R., Jr., 1985. Stratigraphy of the late middle Eocene to early Oligocene in the Bath Cliff section Barbados, West Indies. *Micropaleontology*, 30:390–425.
- Sigurdsson, H., Leckie, R.M., Acton, G.D., et al., 1997. *Proc. ODP, Init. Repts.*, 165: College Station, TX (Ocean Drilling Program).

- Vinassa de Regny, P.E., 1900. Radiolari Miocenici Italiani. *Mem. R. Acad. Sci. Inst. Bologna, Ser. 5*, 8:227–257.
- Wise, S.W., and Weaver, F.M., 1973. Origin of cristobalite-rich Tertiary sediments in the Atlantic and Gulf Coastal plain. *Trans. Gulf Coast Assoc. Geol. Soc.*, 23:305–323.
- Zachos, J.C., Lohmann, K.C., Walker, J.C.G., and Wise, S.W., Jr., 1993. Abrupt climate change and transient climates during the Paleogene: a marine perspective. *J. Geol.*, 101:191–213.
- Zittel, K.A., 1876. Ueber einige fossile Radiolarien auf der norddeutschen Kreide. *Z. Dtsch. Geol. Gesell.*, 28:75–86.

**Date of initial receipt: 8 June 1998**

**Date of acceptance: 25 January 1999**

**Ms 165SR-026**

#### APPENDIX 1 TAXONOMIC LIST

- Amphicraspedum murrayanum* Haeckel  
*Amphicraspedum murrayanum* Haeckel, 1887, p. 523, pl. 44, fig. 10; Sanfilippo and Riedel, 1973, p. 524, pl. 10, figs. 3–6, pl. 28, fig. 1
- Amphicraspedum prolixum* Sanfilippo and Riedel, 1973, p. 524, pl. 10, figs. 711, pl. 28, figs. 3, 4
- Anthocystoma* sp. Riedel and Sanfilippo, 1970, p. 524, pl. 6, figs. 2–4
- Artophormis gracilis* Riedel  
*Artophormis gracilis* Riedel, 1959, p. 300, pl. 2, figs. 12–13; Riedel and Sanfilippo, 1970, p. 532, pl. 13, fig. 6; 1971, pl. 3B, figs. 5–7, pl. 6, fig. 7; Sanfilippo and Nigrini, 1995, p. 272, pl. I, figs. 1–5
- Bekoma* spp.  
This species designation comprises indeterminate forms of the following two species:
- Bekoma bidartensis* Riedel and Sanfilippo  
*Bekoma bidartensis* Riedel and Sanfilippo, 1971, p. 1592, pl. 7, figs. 1–7; Foreman, 1973, p. 432, pl. 3, figs. 20–21, pl. 10, fig. 6  
*Bekoma bidartensis* Riedel and Sanfilippo, 1978, p. 65
- Bekoma campechensis* Foreman, 1973, p. 432, pl. 3, fig. 24, pl. 10, figs. 1–2
- Buryella clinata* Foreman  
*Buryella clinata* Foreman, 1973, p. 433, pl. 8, figs. 1–3, pl. 9, fig. 19; Foreman, 1975, p. 620, pl. 9, figs. 35–36
- Buryella pentadica* Foreman, 1973, p. 433, pl. 8, fig. 8, pl. 9, figs. 15–16
- Buryella* spp.  
This species designation is used for indeterminate forms of *B. tetradicula* and *B. pentadica*.
- Buryella tetradicula* Foreman, 1973, p. 433, pl. 8, figs. 4–5, pl. 9, figs. 13–14; Hollis, 1993, p. 323
- Calocyclus bandycia* (Mato and Theyer)  
*Lynchocanoma bandycia* Mato and Theyer, 1980, p. 225, pl. 1, figs. 1–6  
*Calocyclus bandycia* (Mato and Theyer), Sanfilippo and Riedel in Saunders et al., 1985, p. 411, pl. 5, figs. 1, 5–6
- Calocyclus hispida* (Ehrenberg)  
*Anthocytis hispida* Ehrenberg, 1873, p. 216; 1875, pl. 8, fig. 2  
*Calocyclus hispida* (Ehrenberg) Foreman, 1973, p. 434, pl. 1, figs. 12–15, pl. 9, fig. 18
- Calocyclus turris* Ehrenberg  
*Calocyclus turris* Ehrenberg, 1873, p. 218; 1875, pl. 18, fig. 7; Foreman, 1973, p. 434
- Calocyctetta* (*Calocyctetta*) *robusta* Moore  
*Calocyctetta* (*Calocyctetta*) *robusta* Moore, 1971, p. 743, pl. 10, figs. 5–6; Sanfilippo and Riedel, 1992, pp. 28, 36; Sanfilippo and Nigrini, 1995, p. 272, pl. II, figs. 2–3
- Calocyctoma ampulla* (Ehrenberg)  
*Eucyrtidium ampulla* Ehrenberg, 1854, pl. 36, figs. 15a–c; 1873, p. 22
- Calocyctoma ampulla* (Ehrenberg)  
*Calocyctoma ampulla* (Ehrenberg), Foreman, 1973, p. 434, pl. 1, figs. 1–5; 1975, p. 22
- Calocyctoma castum* (Haeckel)  
*Calocyctas casta* Haeckel, 1887, p. 1384, pl. 73, fig. 10  
*Calocyctoma castum* (Haeckel), Foreman, 1973, p. 434, pl. 1, figs. 7, 9, 10
- Carpocanistrum* spp.  
This species designation represents all forms of *Carpocanistrum* observed.
- Centrobotrys gravida* Moore, 1971, p. 744, pl. 5, fig. 8
- Centrobotrys petrushevskaya* Sanfilippo and Riedel  
*Centrobotrys* (?) sp. A Riedel and Sanfilippo, 1971, p. 1602, pl. 3F, figs. 15–16  
*Centrobotrys petrushevskaya* Sanfilippo and Riedel, 1973, p. 532, pl. 36, figs. 12–3
- Ceratospyris articulata* Ehrenberg  
*Ceratospyris articulata* Ehrenberg, 1873, p. 218; 1875, pl. 20, fig. 4; Sanfilippo and Riedel, 1973, p. 526, pl. 15, figs. 1–3, pl. 31, figs. 8, 9
- Cryptocarpium azyx* (Sanfilippo and Riedel)  
*Carpocanistrum azyx* Sanfilippo and Riedel, 1973, p. 530, pl. 35, fig. 9  
*Cryptocarpium azyx* (Sanfilippo and Riedel), Sanfilippo and Riedel, 1992, p. 6, pl. 2, fig. 21
- Cryptocarpium ornatum* (Ehrenberg)  
*Cryptoprora ornata* Ehrenberg, 1873, p. 222; 1875, pl. 5, fig. 8; Sanfilippo et al., 1985, p. 693, figs. 27.2a, b  
*Cryptocarpium ornatum* (Ehrenberg), Sanfilippo and Riedel, 1992, pp. 6 and 36, pl. 2, figs. 18–20
- Cyrtocapsella tetrapera* Haeckel  
*Cyrtocapsa* (*Cyrtocapsella*) *tetrapera* Haeckel, 1887, p. 1512, pl. 78, fig. 5  
*Cyrtocapsella tetrapera* Haeckel, Sanfilippo and Riedel, 1970, p. 453, pl. 1, figs. 16–18; Sanfilippo et al., 1985, p. 670, figs. 16.1a, b; Sanfilippo and Nigrini, 1995, p. 275
- Dendrosprysis fragoides* Sanfilippo and Riedel, 1973, p. 526, pl. 15, figs. 8–13, pl. 31, figs. 13, 14
- Dictyomitra multicostata* Zittel, 1876, p. 81, pl. 2, figs. 2–4
- Dictyophimus craticula* Ehrenberg  
*Dictyophimus craticula* Ehrenberg, 1873, p. 223; 1875, pl. 5, figs. 4, 5; Sanfilippo and Riedel, 1973, p. 529, pl. 19, fig. 1, pl. 33, fig. 11
- Dictyoprora amphora* (Haeckel) grp.  
*Dictyocephalus amphora* in Haeckel, 1887, p. 1305, pl. 62, fig. 4.  
*Dictyoprora amphora* (Haeckel) Nigrini, 1977, p. 250, pl. 4, figs. 1, 2
- Dictyoprora armadillo* (Ehrenberg)  
*Eucyrtidium armadillo* Ehrenberg, 1873, p. 225; 1875, p. 70, pl. 9, fig. 10  
*Theocompe armadillo* (Ehrenberg) grp., Riedel and Sanfilippo, 1971, p. 1601, pl. 3E, figs. 3–5, (partim)  
*Dictyoprora armadillo* (Ehrenberg), Nigrini, 1977, p. 250, pl. 4, fig. 4
- Dictyoprora mongolfieri* (Ehrenberg)  
*Eucyrtidium mongolfieri* Ehrenberg, 1854, pl. 36, fig. 18, B lower; 1873, p. 230  
*Dictyoprora mongolfieri* (Ehrenberg), Nigrini, 1977, p. 250, pl. 4, fig. 7
- Dictyoprora pirum* (Ehrenberg)  
*Eucyrtidium pirum* Ehrenberg, 1873, p. 232; 1875, pl. 10, fig. 14  
*Dictyoprora pirum* (Ehrenberg), Nigrini, 1977, p. 251, pl. 4, fig. 8
- Didymocystis prismatica* (Haeckel)  
*Pipettella prismatica* Haeckel, 1887, p. 305, pl. 39, fig. 6; Riedel, 1959, p. 287, pl. 1, fig. 1  
*Pipettella tuba* Haeckel, 1887, p. 337, pl. 39, fig. 7  
*Cannartus prismaticus* (Haeckel), Riedel and Sanfilippo, 1970, pl. 15, fig. 1  
*Didymocystis prismatica* (Haeckel), Sanfilippo and Riedel, 1980, p. 1010; Sanfilippo and Nigrini, 1995, p. 275
- Dorcosprysis ateuchus* (Ehrenberg)  
*Ceratospyris ateuchus* Ehrenberg, 1873, p. 218; 1875, pl. 21, fig. 4D  
*Cantharosprysis ateuchus* (Ehrenberg), Haeckel, 1887, p. 1051; Riedel, 1959, p. 294, pl. 22, figs. 3–4

- Dorcadospyris ateuchus* (Ehrenberg), Riedel and Sanfilippo, 1970, p. 523, pl. 15, fig. 4; Sanfilippo and Nigrini, 1995, p. 275, pl. III, figs. 2–4
- Dorcadospyris papilio* (Riedel)  
*Hexaspispris papilio* Riedel, 1959, p. 294, pl. 2, figs. 1–2  
*Dorcadospyris papilio* (Riedel), Riedel and Sanfilippo, 1970, p. 523, pl. 15, fig. 5; Sanfilippo and Nigrini, 1995, p. 278, pl. III, fig. 1
- Dorcadospyris pseudopapilio* Moore, 1971, p. 738, pl. 6, figs. 7–8
- Eucyrtidium diaphanes* Sanfilippo and Riedel  
*Calocyclas coronata* Carnevale, 1908, p. 33, pl. 4, fig. 24 (*non Eucyrtidium coronatum* Ehrenberg, 1873)
- Eucyrtidium diaphanes* Sanfilippo and Riedel, Sanfilippo et al., 1973, p. 221, pl. 5, figs. 12–14 (new name); Sanfilippo and Nigrini, 1995, p. 278, pl. I, figs. 6–11
- Eusyringium fistuligerum* (Ehrenberg)  
*Eucyrtidium fistuligerum* Ehrenberg, 1873, p. 229; 1875, pl. 9, fig. 3.  
*Eusyringium fistuligerum* (Ehrenberg), Riedel and Sanfilippo, 1970, p. 527, pl. 8, figs. 8–9
- Eusyringium lagena* (Ehrenberg)  
*Lithopera lagena* Ehrenberg, 1873, p. 241; 1875, pl. 3, fig. 4  
*Eusyringium lagena* (Ehrenberg), Riedel and Sanfilippo, 1970, p. 527, pl. 8, figs. 5–7; Foreman, 1973, p. 436, pl. 11, figs. 4–5; Sanfilippo et al., 1985, p. 672, figs. 17.2a–c
- Giraffospiris lata* Goll, 1969, p. 334, pl. 58, figs. 22, 24–26
- Lamptonium fabaeforme chaunothorax* Riedel and Sanfilippo  
*Lamptonium* (?) *fabaeforme* (?) *chaunothorax* Riedel and Sanfilippo, 1970, p. 524, pl. 5, figs. 8–9  
*Lamptonium fabaeforme constrictum* Riedel and Sanfilippo  
*Lamptonium* (?) *fabaeforme* (?) *constrictum* Riedel and Sanfilippo, 1970, p. 523, pl. 5, fig. 7
- Lamptonium fabaeforme fabaeforme* (Krasheninnikov)  
(?) *Cyrtocalpis fabaeformis* Krasheninnikov, 1960, p. 296, pl. 3, fig. 11  
*Lamptonium* (?) *fabaeforme fabaeforme* (Krasheninnikov), Riedel and Sanfilippo, 1970, p. 523, pl. 5, fig. 6; Foreman, 1973, p. 436, pl. 6, figs. 6–9
- Lamptonium pennatum* Foreman, 1973, p. 436, pl. 6, figs. 3–5, pl. 11, fig. 13
- Lithochytris vespertilio* Ehrenberg  
*Lithochytris vespertilio* Ehrenberg, 1873, p. 239; 1875, pl. 4, fig. 10; Riedel and Sanfilippo, 1971, p. 528, pl. 9, figs. 8, 9
- Lithochytris archaea* Riedel and Sanfilippo, 1970, p. 528, pl. 9, fig. 7; 1971, pl. 7, fig. 13
- Lithocyctlia angusta* (Riedel)  
*Trigonactura* (?) *angusta* Riedel, 1959, p. 292, pl. 1, fig. 6  
*Lithocyctlia angustum* (Riedel), Riedel and Sanfilippo, 1970, p. 522, pl. 13, figs. 1–2  
*Lithocyctlia angusta* (Riedel) Sanfilippo and Riedel, 1973, p. 523; Sanfilippo et al., 1985, p. 653, figs. 7.3a–c
- Lithocyctlia aristotelis* (Ehrenberg) grp.  
*Astromma aristotelis* Ehrenberg, 1847, p. 55, fig. 10  
*Lithocyctlia aristotelis* (Ehrenberg) grp., Riedel and Sanfilippo, 1970, p. 522, pl. 13, figs. 1–2
- Lithocyctlia ocellus* Ehrenberg grp.  
*Lithocyctlia ocellus* Ehrenberg, 1854, pl. 36, figs. 30; 1873, p. 240  
*Lithocyctlia ocellus* Ehrenberg grp., Riedel and Sanfilippo, 1970, p. 522, pl. 5, figs. 1–2
- Lophocyrtis biaurita* (Ehrenberg)  
*Eucyrtidium biaurita* Ehrenberg, 1873, p. 226; 1875, p. 70, pl. 10, figs. 7, 8
- Lophocyrtis biaurita* (Ehrenberg), Haeckel, 1887, p. 1411; Cita, Nigrini and Gartner, 1970, p. 404, pl. 2, figs. I–K
- Lophocyrtis* (*Cyclampterium*) *milowi* (Riedel and Sanfilippo)  
*Cyclampterium* (?) *milowi* Riedel and Sanfilippo, 1971, p. 1593, pl. 3B, fig. 3, pl. 7, figs. 8–9; Ling, 1975, p. 731, pl. 12, fig. 15  
*Cyclampterium milowi* Riedel and Sanfilippo, 1978, p. 67, pl. 4, fig. 14
- Lophocyrtis* (*Cyclampterium*) *milowi* (Riedel and Sanfilippo), Sanfilippo, 1990, p. 306, pl. I, figs. 13–16, pl. II, figs. 1, 2
- Lophocyrtis* (*Cyclampterium*) *pegetrum* (Sanfilippo and Riedel)  
*Cyclampterium* (?) *pegetrum* Sanfilippo and Riedel, 1970, p. 456, pl. 2, figs. 8–10; Goll, 1972, p. 959, pl. 24, figs. 1–4, pl. 25, figs. 1–3  
*Cyclampterium pegetrum* Riedel and Sanfilippo, 1978, p. 68, pl. 4, fig. 16  
*Lophocyrtis* (*Cyclampterium*) *pegetrum* (Sanfilippo and Riedel), Sanfilippo, 1990, p. 307, pl. II, figs. 3–5
- Lophocyrtis* (*Cyclampterium*) spp.  
This species designation is used for indeterminate forms of *Lophocyrtis* (*Cyclampterium*) *milowi* and *Lophocyrtis* (*Cyclampterium*) *pegetrum*.
- Lychnocanoma amphitrite* Foreman, 1973, p. 437, pl. 11, fig. 10
- Lychnocanoma auxilla* Foreman, 1973, p. 437, pl. 2, fig. 6, pl. 11, figs. 1, 2
- Lychnocanoma babylonis* (Clark and Campbell) grp.  
*Dictyophimus babylonis* Clark and Campbell, 1942, p. 67, pl. 9, figs. 32, 36  
*Lychnocanoma babylonis* (Clark and Campbell) grp. Foreman, 1973, p. 437, pl. 2, fig. 1
- Lychnocanoma bajunensis* Renz, 1984, p. 459, pl. 1, figs. 4–6
- Lychnocanoma bellum* (Clark and Campbell)  
*Lychnocanum bellum* Clark and Campbell, 1942, p. 72, pl. 9, figs. 35, 39; Riedel and Sanfilippo, 1970, p. 529, pl. 10, fig. 5; Riedel and Sanfilippo, 1971, p. 1595  
*Lychnocanoma bellum* (Clark and Campbell), Foreman, 1973, p. 437, pl. 1, fig. 17, pl. 11, fig. 9
- Lychnocanoma* (?) *costata* Nishimura, 1992, p. 342, pl. 6, figs. 4–6
- Lychnocanoma* (?) *pileus* Nishimura, 1992, p. 344, pl. 6, figs. 7, 8; pl. 13, fig. 5
- Lychnocanoma elongata* (Vinassa de Regny)  
*Tetrahedrina elongata* Vinassa de Regny, 1900, p. 243, pl. 2, fig. 31  
*Lychnocanum bipes* Riedel, 1959, p. 294, pl. 2, figs. 56  
*Lychnocanoma elongata* (Vinassa de Regny), Sanfilippo et al., 1973, p. 221, pl. 5, figs. 19–20; Sanfilippo and Nigrini, 1995, p. 282, pl. IV, fig. 11
- Orbula comitata* Foreman, 1973, p. 437, pl. 3, fig. 11; pl. 10, figs. 7, 8
- Phormocyrtis cubensis* (Riedel and Sanfilippo)  
*Eucyrtidium cubense* Riedel and Sanfilippo, 1971, p. 1594, pl. 7, figs. 10–11  
*Phormocyrtis cubensis* (Riedel and Sanfilippo), Foreman, 1973, p. 438, pl. 7, figs. 11–12, 14
- Phormocyrtis striata exquisita* (Kozlova)  
*Podocyrtis exquisita* Kozlova in Kozlova and Gorbovets, 1966, p. 106, pl. 17, fig. 2  
*Phormocyrtis striata exquisita* (Kozlova), Foreman, 1973, p. 438, pl. 7, figs. 1–4, 7–8, pl. 12, fig. 5
- Phormocyrtis striata praexquisita* Nishimura, 1992, p. 346, pl. 9, figs. 1–3
- Phormocyrtis striata striata* Brandt  
*Phormocyrtis striata* Brandt, 1935, p. 55, pl. 9, fig. 12; Riedel and Sanfilippo, 1970, p. 532, pl. 10, fig. 7  
*Phormocyrtis striata striata* Brandt, Foreman, 1973, p. 438, pl. 7, figs. 5–6, 9
- Phormocyrtis turgida* (Krasheninnikov)  
*Lithocampe turgida* Krasheninnikov, 1960, p. 301, pl. 3, fig. 17  
*Phormocyrtis turgida* (Krasheninnikov), Foreman, 1973, p. 438, pl. 7, fig. 10, pl. 12, fig. 6
- Podocyrtis* (*Lamppterium*) *chalara* Riedel and Sanfilippo  
*Podocyrtis* (*Lamppterium*) *chalara* Riedel and Sanfilippo, 1970, p. 535, pl. 12, figs. 2–3; Riedel and Sanfilippo, 1978, p. 71, pl. 8, fig. 3, text-fig. 3
- Podocyrtis* (*Lamppterium*) *fasciolata* (Nigrini)  
*Podocyrtis* (*Podocyrtis*) *ampla fasciolata* Nigrini, 1974, p. 1069, pl. 1K, figs. 1–2, pl. 4, figs. 2–3  
*Podocyrtis* (*Lamppterium*) *fasciolata* (Nigrini), Sanfilippo et al., 1985, p. 697, fig. 30.7
- Podocyrtis* (*Lamppterium*) *goetheana* (Haeckel)

- Cycladophora goetheana* Haeckel, 1887, p. 1376, pl. 65, fig. 5  
*Podocyrthis (Lampterium) goetheana* (Haeckel), Riedel and Sanfilippo, 1970, p. 535
- Podocyrthis (Lampterium) mitra* Ehrenberg  
*Podocyrthis mitra* Ehrenberg, 1854, pl. 36, fig. B20; 1873, p. 251; *non* Ehrenberg, 1875, pl. 15, fig. 4; *Podocyrthis (Lampterium) mitra*, Riedel and Sanfilippo, 1970, p. 534, pl. 11, figs. 5–6; 1978, text-fig. 3; Sanfilippo et al., 1985, p. 698, fig. 30.10
- Podocyrthis (Lampterium) sinuosa* Ehrenberg  
*Podocytis sinuosa* Ehrenberg, 1873, p. 253; 1875, pl. 15, fig. 5; *Podocyrthis (Lampterium) Sinuosa*, Riedel and Sanfilippo, 1970, p. 534, pl. 11, figs. 3–4; 1978, text-fig. 3; Sanfilippo et al., 1985, p. 698, fig. 30.9
- Podocyrthis (Lampterium) trachodes* Riedel and Sanfilippo, 1970, p. 535, pl. 11, fig. 7, pl. 12, fig. 1; Sanfilippo et al., 1985, p. 699, fig. 30.14
- Podocyrthis (Podocytoges) papalis* Ehrenberg  
*Podocytis papalis* Ehrenberg, 1847, p. 55, fig. 2; *Podocyrthis (Podocytoges) papalis*, Riedel and Sanfilippo, 1970, p. 533, pl. 11, fig. 1; Sanfilippo and Riedel, 1973, p. 531, pl. 20, figs. 11–14, pl. 36, figs. 2–3
- Podocyrthis (Podocytoges) ampla* Ehrenberg  
*Podocytis (?) ampla* Ehrenberg, 1873, p. 248; 1875, pl. 16, fig. 7; Riedel and Sanfilippo, 1970, p. 533, pl. 12, figs. 7–8  
*Podocyrthis (Podocytoges) ampla* Ehrenberg, Sanfilippo and Riedel, 1992, p. 14, pl. 5, fig. 4
- Podocyrthis (Podocytoges) diamesa* Riedel and Sanfilippo  
*Podocytis (Podocyrthis) diamesa* Riedel and Sanfilippo, 1970, p. 533 (pars), pl. 12, fig. 4, *non* figs. 5–6; Sanfilippo and Riedel, 1973, p. 531, pl. 20, figs. 9–10, pl. 35, figs. 10–11  
*Podocytis (Podocytoges) diamesa* Sanfilippo and Riedel, 1992, p. 14
- Pterocodon ampla* (Brandt)  
*Theocyrtis ampla* Brandt, 1935, p. 56, pl. 9, figs. 13–15  
*Pterocodon (?) ampla* (Brandt), Foreman, 1973, p. 438, pl. 5, figs. 3–5
- Rhabdolithis pipa* Ehrenberg, 1854, pl. 36, fig. 59; 1875, p. 159, pl. 1, fig. 27.
- Rhopalocanium ornatum* Ehrenberg  
*Rhopalocanium ornatum* Ehrenberg, 1847, fig. 3; 1854, pl. 36, fig. 9; 1873, p. 256; 1875, pl. 17, fig. 8; Foreman, 1973, p. 439, pl. 2, figs. 8–10, pl. 12, fig. 3
- Sethochytris triconicus* Haeckel  
(?) *Sethochytris triconicus* Haeckel, 1887, p. 1239, pl. 57, fig. 13; Riedel and Sanfilippo, 1970, p. 528, pl. 9, figs. 5–6; Sanfilippo et al., 1985, p. 680, figs. 22.1a–d
- Spongatractus balbis* Sanfilippo and Riedel, 1973, p. 518, pl. 2, figs. 1–3, pl. 25, figs. 1–2
- Spongatractus pachystylus* (Ehrenberg)  
*Spongosphera pachystyla* Ehrenberg, 1873, p. 256; 1875, pl. 26, fig. 3  
*Spongatractus pachystylus* (Ehrenberg), Sanfilippo and Riedel, 1973, p. 519, pl. 2, figs. 4–6, pl. 25, fig. 3
- Spongodiscus americanus* Kozlova  
*Spongodiscus americanus* Kozlova, Kozlova and Gorbovets, 1966, p. 88, pl. 14, figs. 1,2; Sanfilippo and Riedel, 1973, p. 524, pl. 11, figs. 9–13, pl. 27, fig. 11, pl. 28, fig. 9
- Spongodiscus cruciferus* (Clark and Campbell)  
*Spongasteriscus cruciferus* Clark and Campbell, 1942, p. 50, pl. 1, figs. 1–6,8,10,11,16–18  
*Spongodiscus cruciferus* (Clark and Campbell), Sanfilippo and Riedel, 1973, p. 524, pl. 11, figs. 14–17, pl. 28, figs. 10, 11
- Spongodiscus quartus* (Borisenko)  
*Stauropolyx quartus* Borisenko, 1958, pl. 2, fig. 5  
*Spongodiscus quartus* (Borisenko), Sanfilippo and Riedel, 1973, p. 525, pl. 12, figs. 6,7, pl. 29, figs. 5, 6
- Stichomitra granulata* (Petrushevskaya)  
*Lithocampe* sp. A Dumitrica, 1973, p. 789, pl. 10, fig. 3, pl. 11, fig. 3  
*Lithocampe (?) granulata* Petrushevskaya, 1977, p. 18, pl. 3a, b, v  
*Stichomitra granulata* (Petrushevskaya), Hollis, 1993, p. 321, pl. I, figs. 10–11
- Stylostrochus alveatus* Sanfilippo and Riedel, 1973, p. 525, pl. 13, figs. 4, 5, pl. 30, figs. 3, 4
- Stylostrochus nitidus* Sanfilippo and Riedel, 1973, p. 525, pl. 13, figs. 9–14, pl. 30, figs. 7–10
- Stylostrochus quadibrachiatus* *quadibrachiatus* Sanfilippo and Riedel, 1973, p. 526, pl. 14, figs. 1, 2, pl. 31, fig. 1
- Theocorys anaclasta* Riedel and Sanfilippo  
*Theocorys anaclasta* Riedel and Sanfilippo, 1970, p. 530, pl. 10, figs. 2–3; Riedel and Sanfilippo, 1978, p. 76, pl. 1, figs. 6–8; Sanfilippo et al., 1985, p. 683, figs. 24.1a–d
- Theocorys anapographa* Riedel and Sanfilippo, 1970, p. 530, pl. 10, fig. 4
- Theocorys (?) phyzella* Foreman, 1973, p. 440, pl. 5, fig. 8, pl. 12, fig. 1
- Theocorys spongoconus* Kling, 1971, p. 1087, pl. 5, fig. 6
- Theocotyle conica* Foreman  
*Theocotyle (Theocotyle) cryptocephala* (?) *conica* Foreman, 1973, p. 440, pl. 4, fig. 11, pl. 12, figs. 19–20  
*Theocotyle conica* Foreman, Sanfilippo, and Riedel, 1982, p. 177, pl. 2, fig. 13
- Theocotyle cryptocephala* (Ehrenberg)  
(?) *Eucyrtidium cryptocephalum* Ehrenberg, 1873, p. 227; 1875, pl. 11, fig. 11  
*Theocotyle cryptocephala* (Ehrenberg), Sanfilippo and Riedel, 1982, p. 178, pl. 2, figs. 4–7
- Theocotyle nigriniae* Riedel and Sanfilippo  
*Theocotyle cryptocephala* (?) *nigriniae* Riedel and Sanfilippo, 1970, p. 525, pl. 6, fig. 5 (*non* fig. 6)  
*Theocotyle nigriniae* Riedel and Sanfilippo, Sanfilippo and Riedel, 1982, p. 178, pl. 2, figs. 1–3
- Theocotylissa alpha* Foreman  
*Theocotyle (Theocotylissa) alpha* Foreman, 1973, p. 441, pl. 4, figs. 13–15 (*non* 14), pl. 12, fig. 16; Foreman, 1975, p. 621  
*Theocotylissa alpha* Foreman, Sanfilippo and Riedel, 1982, p. 179, pl. 2, figs. 16–17
- Theocotylissa auctor* Foreman  
*Theocotyle (Theocotylissa) auctor* Foreman, 1973, p. 441, pl. 4, figs. 8–10, pl. 12, fig. 13  
*Theocotylissa auctor* Foreman, Sanfilippo, and Riedel, 1982, p. 180, pl. 2, figs. 14, 15
- Theocotylissa ficus* (Ehrenberg)  
*Eucyrtidium ficus* Ehrenberg 1873, p. 228; 1875, pl. 11, fig. 19  
*Theocotylissa ficus* (Ehrenberg), Sanfilippo and Riedel, 1982, p. 180, pl. 2, figs. 19–20
- Theocyrtis annosa* (Riedel)  
*Phormocytis annosa* Riedel, 1959, p. 295, pl. 2, fig. 7  
*Calocyctella annosa* (Riedel) Petrushevskaya and Kozlova, 1972, p. 544  
*Theocyrtis annosa* (Riedel) Riedel and Sanfilippo, 1970, p. 535, pl. 15, fig. 9; Sanfilippo et al., 1985, p. 701, figs. 32.2a, b; Sanfilippo and Nigrini, 1995, p. 282, pl. IV, figs. 1–4
- Theocyrtis tuberosa* Riedel, *emend.* Sanfilippo et al.  
*Theocyrtis tuberosa* Riedel, 1959, p. 298, pl. 2, figs. 10–11; Sanfilippo et al., 1985, p. 701, figs. 32.1a–d
- Thrysocystis (Pentalacorys) lochites* Sanfilippo and Riedel, 1982, p. 175, pl. 1, fig. 13, pl. 3, figs. 5–9
- Thrysocystis (Pentalacorys) tensa* Foreman  
*Thrysocystis hirsuta* Foreman, 1973, p. 442, pl. 3, figs. 13–16, pl. 12, fig. 8  
*Thrysocystis (Pentalacorys) tensa* Foreman, Sanfilippo and Riedel, 1982, p. 176, pl. 1, figs. 6–7, pl. 3, figs. 1–2
- Thrysocystis (Pentalacorys) tetricantha* (Ehrenberg)  
*Podocyrthis tetricantha* Ehrenberg, 1873, p. 254; 1875, pl. 13, fig. 2  
*Thrysocystis (Pentalacorys) tetricantha* (Ehrenberg), Sanfilippo and Riedel, 1982, p. 176, pl. 1, figs. 11–12, pl. 3, fig. 10
- Thrysocystis (Pentalacorys) triacantha* (Ehrenberg)  
*Podocyrthis triacantha* Ehrenberg, 1873, p. 254; 1875, pl. 13, fig. 4

- Thyrsocyrtis (Pentalacorys) triacantha* (Ehrenberg), Sanfilippo and Riedel, 1982, p. 176, pl. 1, figs. 8–10, pl. 3, figs. 3–4
- Thyrsocyrtis (Thyrsocyrtis) bromia* Ehrenberg  
*Thyrsocyrtis bromia* Ehrenberg, 1873, p. 260; 1875, pl. 12, fig. 2; Sanfilippo and Riedel, 1982, p. 172, pl. 1, figs. 17–20
- Thyrsocyrtis (Thyrsocyrtis) hirsuta* (Krasheninnikov)  
*Podocyrtis hirsutus* Krasheninnikov, 1960, p. 300, pl. 3, fig. 16
- Thyrsocyrtis (Thyrsocyrtis) hirsuta* (Krasheninnikov), Riedel and Sanfilippo, 1970, p. 526, pl. 7, figs. 8, 9
- Thyrsocyrtis (Thyrsocyrtis) hirsuta* (Krasheninnikov), Sanfilippo and Riedel, 1982, p. 173, pl. 1, figs. 3–4
- Thyrsocyrtis (Thyrsocyrtis) rhizodon* Ehrenberg
- Thyrsocyrtis rhizodon* Ehrenberg, 1873, p. 262; 1875, pl. 12, fig. 1; Sanfilippo and Riedel, 1982, p. 173, pl. 1, figs. 14–16, pl. 3, figs. 12–17
- Thyrsocyrtis (Thyrsocyrtis) robusta* Riedel and Sanfilippo  
*Thyrsocyrtis hirsuta robusta* Riedel and Sanfilippo, 1970, p. 526, pl. 8, fig. 1
- Thyrsocyrtis (Thyrsocyrtis) robusta* Riedel and Sanfilippo, Sanfilippo and Riedel, 1982, p. 174, pl. 1, fig. 5
- Tripocalpis cassidus* Nishimura, 1992, p. 330, pl. 3, fig. 8; pl. 12, fig. 12
- Tristylospyris triceros* (Ehrenberg)  
*Ceratospyris triceros* Ehrenberg, 1873, p. 220; 1875, pl. 21, fig. 5  
*Tristylospyris triceros* (Ehrenberg), Haeckel, 1887, p. 1033; Riedel, 1959, p. 292, pl. 1, figs. 7–8; Sanfilippo et al., 1985, p. 665, figs. 10.3a, b



Plate 1. Scale bar for fig. 1 = 100 µm; scale bar for figs. 2–17 = 100 µm. Codes after sample description are slide description and England Finder coordinates, respectively. **1.** Fragmented opaline radiolarians with ash fragments. Sample 165-998A-36X-1, 36–38 cm, ph.1 O40/0. **2.** *Thrysocyrtis (Pentalacorys) tetracantha*. Fragmented, partially dissolved form. Sample 165-998B-6R-3, 26–28 cm, sl.2 D8/1. **3.** Clay-filled radiolarian test showing partial dissolution and replacement of silica. Sample 165-998B-22R-1, 36–38 cm, ph.2 M42/0. **4.** Siliceous mold of a radiolarian. Sample 165-998B-22R-1, 36–38 cm, ph.2 M39/0. **5–7, 11.** Forms showing strong signs of dissolution particularly in the upper part of the test. Sample 165-998B-34R-1, 35–37 cm, sl.4. (5) O28/0; (6) W8/0; (7) J42/2; (11) W9/0. **8.** *Sethochytris triconiscus*. Morphologically distinctive form even when preservation is less than ideal. Sample 165-998B-17R-3, 37–39 cm, sl.2 H24/1. **9.** *Dictyopora* sp. Early stage of internal mold formation. Parts of original shell wall still intact. Sample 165-998B-23R-5, 45–47 cm, cs.2 T45/0. **10.** *Dictyopora mongolfieri*. The refractive index of radiolarians lower than normal. Note also common siliceous molds of small foraminifers. Sample 165-998B-26R-1, 34–36 cm, sl.4 C25/0. **12.** *Podocyrtis (Lampterium) mitra*. Severely dissolved test in which pore bars are thin or absent. Sample 165-998B-20R-3, 38–39 cm, cs.1 N40/0. **13, 16, 17.** *Thrysocyrtis (Pentalacorys) triacantha*. Tests infilled with clay matrix and severely dissolved. Notice thinning of pore bars and distal appendages. Sample 165-998B-23R-5, 45–47 cm, cs.2 K19/4, K35/0, O9/4. **14.** *Thrysocyrtis (Thrysocyrtis) rhizodon*. Strongly dissolved skeleton partly enclosed in clay matrix. Sample 165-998B-23R-5, 45–47 cm, cs.2 L39/3. **15.** *Lithochytris vespertilio*. Distinctive morphological shape facilitates identification despite poor preservation. Sample 165-998B-23R-5, 45–47 cm, cs.2 H10/0.

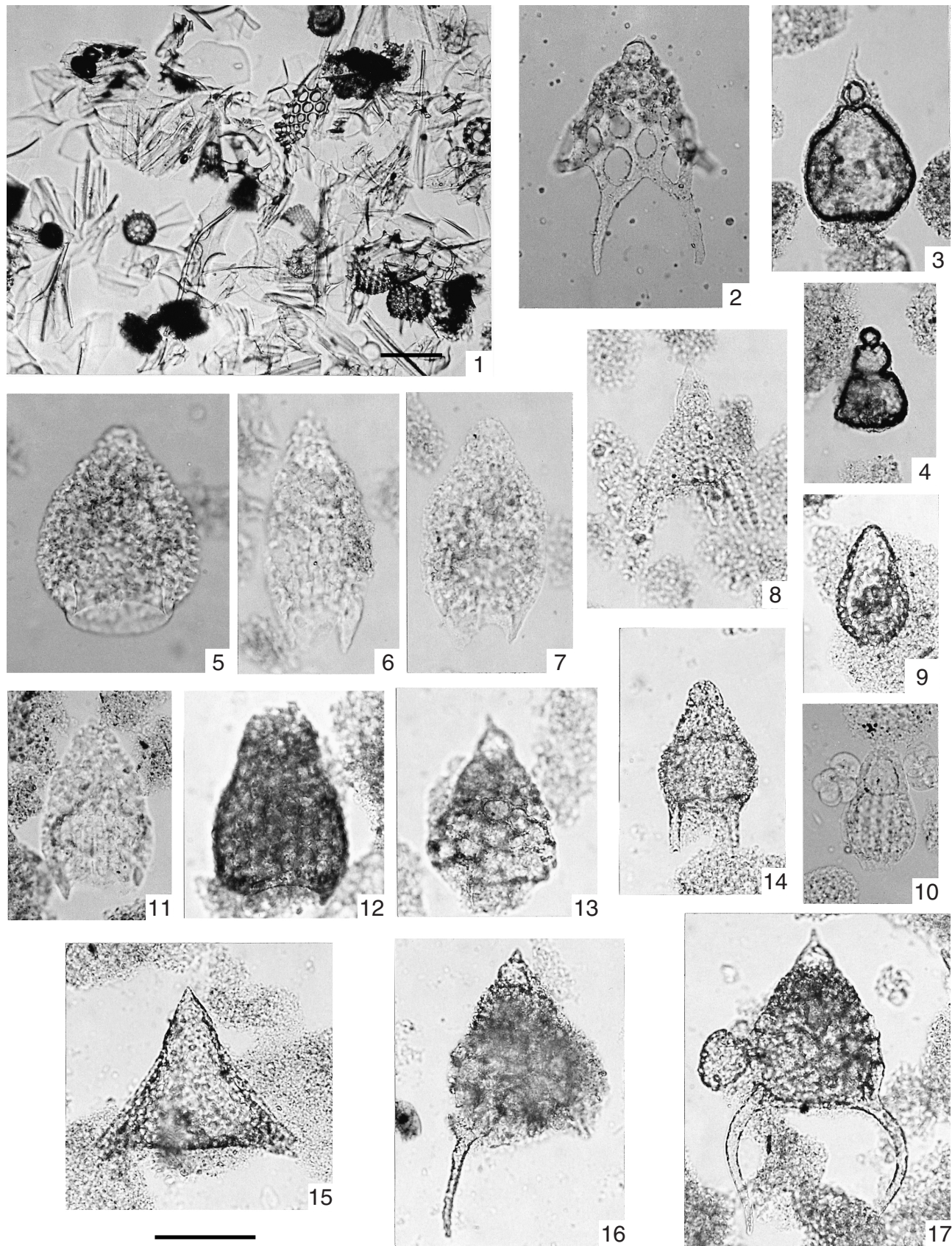




Plate 2. Scale bar for fig. 12 = 100 µm; scale bar for figs. 1–11, 13–17 = 100 µm. Codes after sample description are slide description and England Finder coordinates, respectively. **1.** Fragments of siliceous microfossils, ash fragments, and opaque mineral grains outlining foraminifer skeletons. Sample 165-999B-15R-1, 24–26 cm, sl.4 F36/4. **2.** *Eusyringium fistuligerum*. Relatively robust form. Sample 165-999B-36R-4, 7–9 cm, sl.1 Q26/4. **3.** *Eusyringium fistuligerum*. Strongly corroded but identifiable from distinctive morphology. Sample 165-33R-1, 78–80 cm, cs.1 T30/0. **4–6.** *Carpocanistrum azyx*. Progressive dissolution from a few pore bars (4) to a significant part of the test (6). Sample 165-999B-28R-1, 0–2 cm, sl.3 T2/3, Q7/0, T17/1. **7.** Severely corroded radiolarian skeletons and ash fragments. Sample 165-999B-28R-1, 0–2 cm, sl.3 R5/3. **8.** *Phacodiscid* sp. Cortical shell strongly fragmented because of in situ dissolution. Sample 165-999B-29R-5, 72–74 cm, cs.2 Q32/0. **9.** *Dictyopora mongolfieri*. Note good state of preservation. Sample 165-999B-28R-1, 0–2 cm, sl.3 Q1/3. **10.** *Lithochytris vespertilio*. From one of the better preserved assemblages containing forms commonly unaffected by dissolution together with numerous forms in a stage of dissolution resembling the illustration. Sample 165-999B-35R-1, 73–75 cm, cs.1 C12/3. **11.** *Podocyrtis (Podocyrtis) papalis*. Dissolution in collar region and distal part of thorax. Sample 165-999B-29R-1, 40–46 cm, ph.1 V42/2. **12.** *Calocyclas* sp. Sample contains abundant ash and strongly dissolved radiolarian tests. Sample 165-999B-28R-1, 0–2 cm, sl.3 X17/4. **13.** *Podocyrtis (Lampterium) trachodes*. Test showing strong signs of dissolution in the proximal part of the skeleton. Sample 165-999B-35R-1, 73–75 cm, cs.2 N22/2. **14–17.** *Lithocyclia ocellus*. Progression of dissolution stages in the same sample from moderately well-preserved (14) to an almost unrecognizable form (17). Unless this progression can be recognized, it is impossible to identify forms such as that illustrated in (17). Sample 165-999B-35R-1, 73–75 cm, cs.2 D9/0; G10/3; K41/0; G11/0.

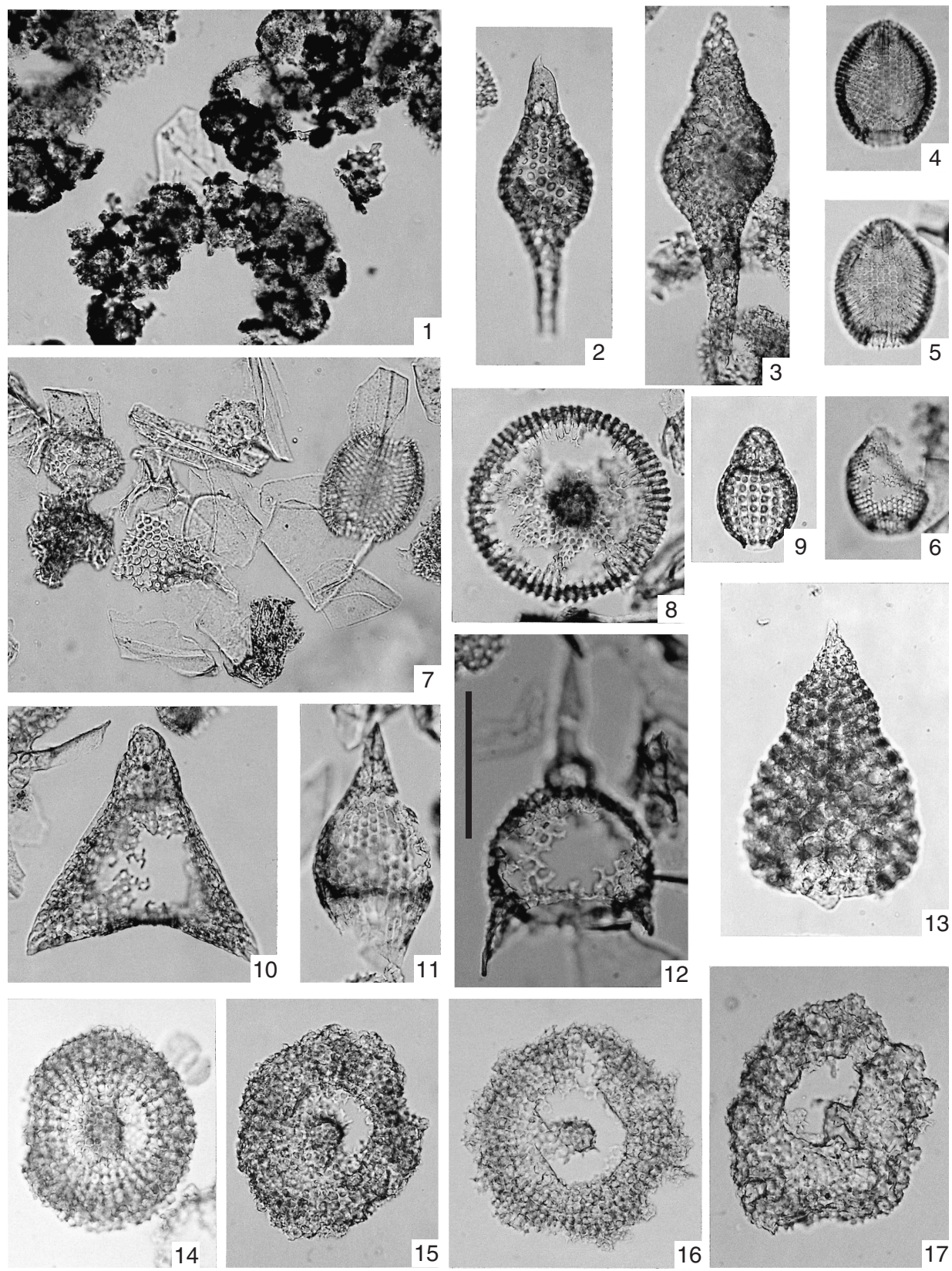




Plate 3. Scale bar for figs. 1–13 = 100 µm. Codes after sample description are slide description and England Finder coordinates, respectively. Distinctive external morphologies or features allow for identification of taxa despite various preservation problems. **1, 2.** *Bekoma campechensis*. (1) Clay-filled and slightly corroded specimen. Note corrosion on left appendage. (2) In this assemblage most specimens belonging to the genus *Bekoma* are represented only by the characteristic cephalic structure. Sample 165-1001A-35R-1, 145–147 cm, sl.4 R41/4, G27/0. **3.** (?) *Buryella tetradiaca*. Strongly corroded and partially infilled fragment. Sample 165-1001A-27R-3, 86–88 cm, ph.4 J9/2. **4.** *Phormocyrtis striata exquisita*. Clay-filled specimen. Sample 165-1001A-27R-3, 86–88 cm, ph.4 O10/3. **5.** *Phormocyrtis cubensis*. Clay-filled specimen. Sample 165-1001A-27R-3, 86–88 cm, cs.1 P37/0. **6, 7.** *Podocyrtis (Podocyrtis) papalis*. Moderately well-preserved specimen (6) and a badly corroded one (7). Sample 165-1001A-27R-3, 86–88 cm, cs.1 S33/4, X17/2. **8.** (?) *Theocorys phyzella*. Characteristic hyaline peristome is dissolved. Sample 165-1001A-27R-3, 86–88 cm, cs.1 N20/4. **9.** *Phormocyrtis turgida*. Despite repeated cleanings, some clay matrix often remains attached to radiolarians. Sample 165-1001A-27R-3, 86–88 cm, cs.1 V5/4. **10.** Opaline fragment of delicate radiolarian. Sample 165-1001A-27R-3, 86–88 cm, ph.1 R8/2. **11–13.** *Amphicraspedium murrayanum*. (11, 12) = forms from the same assemblage that have undergone less diagenesis; (13) = a spongy radiolarian skeleton totally replaced by clay. Sample 165-1001A-27R-1, 108–110 cm, cs.3 U5/2, X17/3, F36/2.

